BRL-TR-3080

DTIC FILE COPY

(4)

TECHNICAL REPORT BRL-TR-3080

BRL

AD-A219 374

LARGE-SCALE SIMULATIONS OF MONOLITHIC AND SEGMENTED PROJECTILES IMPACTING SPACED ARMOR

DANIEL R. SCHEFFLER
THOMAS M. SHERRICK

FEBRUARY 1990

U.S. ARMY LABORATORY COMMAND

BALLISTIC RESEARCH LABORATORY
ABERDEEN PROVING GROUND, MARYLAND

DESTRUCTION NOTICE

Destroy this report when it is no longer needed. DO NOT return it to the originator.

Additional copies of this report may be obtained from the National Technical Information Service, U.S. Department of Commerce, 5285 Port Royal Road, Springfield, VA 22161.

The findings of this report are not to be construed as an official Department of the Army position, unless so designated by other authorized documents.

The use of trade names or manufacturers' names in this report does not constitute indorsement of any commercial product.

REPORT DOCUMENTATION PAGE

Form Approved
OMB No. 0704-0188

1. AGENCY USE ONLY *(Leave blank)*

2. REPORT DATE
February 1990

3. REPORT TYPE AND DATES COVERED
Final, June 88 to present

4. TITLE AND SUBTITLE
Large-Scale Simulations of Monolithic and Segmented Projectiles Impacting Spaced Armor

5. FUNDING NUMBERS

6. AUTHOR(S)
Scheffler, Daniel R., and Sherrick, Thomas M.

7. PERFORMING ORGANIZATION NAME(S) AND ADDRESS(ES)

8. PERFORMING ORGANIZATION REPORT NUMBER

9. SPONSORING/MONITORING AGENCY NAME(S) AND ADDRESS(ES)
US Army Ballistic Research Laboratory
ATTN: SLCBR-DD-T
Aberdeen Proving Ground, MD 21005-5066

10. SPONSORING/MONITORING AGENCY REPORT NUMBER
BRL-TR-3080

11. SUPPLEMENTARY NOTES

12a. DISTRIBUTION/AVAILABILITY STATEMENT
Approved for public release; distribution is unlimited.

12b. DISTRIBUTION CODE

13. ABSTRACT *(Maximum 200 words)*

Numerical simulations are presented describing the performance of segmented and monolithic kinetic energy penetrators against oblique-spaced rolled homogeneous armor (RHA) plates. The three-dimensional simulations depict the effects of striking velocity; target plate thickness-to-penetrator diameter ratio (T/D); segment spacing-to-penetrator diameter ratio (S/D); and the number of segments, on penetrator performance. Keywords:

14. SUBJECT TERMS
kinetic energy penetrator, rolled homogeneous armor, RHA, segmented penetrator, spaced armor, impact, computer simulations, penetration, perforation, kinetic energy, armor

15. NUMBER OF PAGES
66

16. PRICE CODE

17. SECURITY CLASSIFICATION OF REPORT	18. SECURITY CLASSIFICATION OF THIS PAGE	19. SECURITY CLASSIFICATION OF ABSTRACT	20. LIMITATION OF ABSTRACT
UNCLASSIFIED	UNCLASSIFIED	UNCLASSIFIED	UL

NSN 7540-01-280-5500

Standard Form 298 (Rev. 2-89)
Prescribed by ANSI Std. Z39-18
298-102

GENERAL INSTRUCTIONS FOR COMPLETING SF 298

The Report Documentation Page (RDP) is used in announcing and cataloging reports. It is important that this information be consistent with the rest of the report, particularly the cover and title page. Instructions for filling in each block of the form follow. It is important to *stay within the lines* to meet *optical scanning requirements*.

Block 1. Agency Use Only (*Leave blank*).

Block 2. Report Date. Full publication date including day, month, and year, if available (e.g. 1 Jan 88). Must cite at least the year.

Block 3. Type of Report and Dates Covered. State whether report is interim, final, etc. If applicable, enter inclusive report dates (e.g. 10 Jun 87 - 30 Jun 88).

Block 4. Title and Subtitle. A title is taken from the part of the report that provides the most meaningful and complete information. When a report is prepared in more than one volume, repeat the primary title, add volume number, and include subtitle for the specific volume. On classified documents enter the title classification in parentheses.

Block 5. Funding Numbers. To include contract and grant numbers; may include program element number(s), project number(s), task number(s), and work unit number(s). Use the following labels:

C - Contract		PR - Project
G - Grant		TA - Task
PE - Program Element		WU - Work Unit Accession No.

Block 6. Author(s). Name(s) of person(s) responsible for writing the report, performing the research, or credited with the content of the report. If editor or compiler, this should follow the name(s).

Block 7. Performing Organization Name(s) and Address(es). Self-explanatory.

Block 8. Performing Organization Report Number. Enter the unique alphanumeric report number(s) assigned by the organization performing the report.

Block 9. Sponsoring/Monitoring Agency Name(s) and Address(es). Self-explanatory.

Block 10. Sponsoring/Monitoring Agency Report Number. *(If known)*

Block 11. Supplementary Notes. Enter information not included elsewhere such as: Prepared in cooperation with...; Trans. of...; To be published in.... When a report is revised, include a statement whether the new report supersedes or supplements the older report.

Block 12a. Distribution/Availability Statement. Denotes public availability or limitations. Cite any availability to the public. Enter additional limitations or special markings in all capitals (e.g. NOFORN, REL, ITAR).

- DOD - See DoDD 5230.24, "Distribution Statements on Technical Documents."
- DOE - See authorities.
- NASA - See Handbook NHB 2200.2.
- NTIS - Leave blank.

Block 12b. Distribution Code.

- DOD - Leave blank.
- DOE - Enter DOE distribution categories from the Standard Distribution for Unclassified Scientific and Technical Reports.
- NASA - Leave blank.
- NTIS - Leave blank.

Block 13. Abstract. Include a brief *(Maximum 200 words)* factual summary of the most significant information contained in the report.

Block 14. Subject Terms. Keywords or phrases identifying major subjects in the report.

Block 15. Number of Pages. Enter the total number of pages.

Block 16. Price Code. Enter appropriate price code *(NTIS only)*.

Blocks 17. - 19. Security Classifications. Self-explanatory. Enter U.S. Security Classification in accordance with U.S. Security Regulations (i.e., UNCLASSIFIED). If form contains classified information, stamp classification on the top and bottom of the page.

Block 20. Limitation of Abstract. This block must be completed to assign a limitation to the abstract. Enter either UL (unlimited) or SAR (same as report). An entry in this block is necessary if the abstract is to be limited. If blank, the abstract is assumed to be unlimited.

TABLE OF CONTENTS

INTENTIONALLY LEFT BLANK.

LIST OF FIGURES

INTENTIONALLY LEFT BLANK.

ACKNOWLEDGEMENTS

The authors wish to thank the reviewers, Dr. Ennis F. Quigley and Mr. Kent D. Kimsey, for their helpful comments and suggestions in preparing this report. Special thanks go to Mrs. Brenda L. Tucker and Miss Melissa A. Boone who prepared the manuscript.

INTENTIONALLY LEFT BLANK.

1. INTRODUCTION

Within the last several years there has been a lot of interest in the performance of segmented kinetic energy penetrators at velocities greater than 2 km/s. Both experimental and analytical investigations of the penetration mechanisms have been conducted. For example, in 1981 V. Kucher[1], conducted 2-D simulations of a segmented projectile that showed improved performance for segmented projectiles and improved performance with increased segment spacing. Since then, several computer studies have been conducted, among them W. de Rosset and K. D. Kimsey[2], D. R. Scheffler[3], and R. T. Sedgwick and co-workers[4], all showed improved penetrator performance for the segmented rod over an equivalent mass and diameter monolithic rod. In addition to computer simulations, experiments conducted by A. Charters[5,6,7,8] and Bell[9] also suggest that segmented penetrators exhibit improved performance.

Numerical simulations are well suited for the study of segmented kinetic energy penetrators. Numerical studies permit the examination of segmented penetrators without the typical problems encountered in ballistic tests such as; alignment of the individual segments, constraints of pre-extended projectile lengths, projectile yaw, structural integrity of the launch package, and synergistic effects of carrier tubes or carrier rods on overall penetration. Thus, simulations can increase our understanding of the penetration phenomenon as well as supplement the limited ballistic test data.

Most of the data in the literature concentrates on the performance of high-velocity segmented kinetic energy penetrators against semi-infinite steel armor. Some ballistic tests of segmented projectiles impacting spaced plate arrays have been conducted; however, the data is sparse. For example, A. Charters[5,6,7,8] conducted a limited number of ballistic tests showing that each segment "punches through" a target plate in an array allowing the remaining segments to pass through undisturbed, each defeating one plate. Since computations are well suited for modeling segmented projectile impacts, a series of three-dimensional simulations have been conducted to characterize the penetration/perforation phenomenon against spaced armor. The projectile impacts were modeled using version 121 of the HULL finite-difference code.

HULL[10,11] is an Eulerian wave propagation code that uses a second order accurate finite-difference scheme. The material advection scheme is first order. The code solves the partial differential equations of continuum mechanics ignoring heat conduction and viscosity terms. The Mie-Gruneisen equation of state is used to model solids. After vaporization occurs, the Gamma Law equation is used to model the gas. Explosives can be modeled using the Jones-Wilkins-Lee equation of state. Material failure models include: maximum principle stress, maximum principle strain, and the Hancock-Mackenzie triaxial failure model[12]. When material failure occurs, a numerically significant void (i.e. air), is introduced in the cell which permits relaxation of the tensile forces. Recompression is permitted.

2. SIMULATION MATRIX

A series of three-dimensional simulations have been conducted to determine the performance of segmented projectiles striking spaced armor. The performance of the segmented projectile is measured relative to an equivalent mass monolithic penetrator. The length-to-diameter ratio, L/D, of the monolithic tungsten alloy (90W-7Ni-3Fe) penetrator is 20, with a total mass of 274 grams. The segmented projectile geometry separates the monolithic rod into N individual segments with the same diameter as the monolithic projectile.

A number of impact conditions have been modeled to characterize the effects of: striking velocity (1.5-4.0 km/s); target thickness-to-penetrator diameter ratio, T/D, (2 and 4); segment spacing-to-penetrator diameter ratio, S/D, (0 to 8); and the number of individual segments, N, (5 and 20) on penetration/ perforation performance. The computational matrix is summarized in the Table 1. For the cases modeled, the target was comprised of two rolled homogeneous armor (RHA) plates with the same T/D ratio and a normal spacing of 50.8 mm at an obliquity of 60 degrees.

Table 1. Computational Matrix (Nominal Projectile Mass 274 grams).

Problem No.	Velocity (km/s)	N*	S/D*	T/D
5.0004	1.5	5	1	2
5.0000	1.5	1	0	2
5.0005	2.0	5	1	2
5.0001	2.0	1	0	2
5.0006	3.0	5	1	2
5.0002	3.0	1	0	2
5.0007	4.0	5	1	2
5.0003	4.0	1	0	2
518.8800	2.0	5	1	4
6.0002	2.0	1	0	4
518.8833	3.0	5	1	4
6.0003	3.0	1	0	4
518.8844	4.0	5	1	4
6.0004	4.0	1	0	4
7.0001	4.0	5	4	4
7.0002	4.0	5	8	4
8.0000	4.0	20	1	4

*NOTE: N = 1 implies a monolithic projectile
D = 10mm constant projectile diameter

In an effort to preserve material interfaces and minimize material diffusion typically encountered in Eulerian codes, a constant subgrid was chosen for the x-y plane covering a region two diameters away from the penetrator. The constant subgrid provides six cells across the diameter of the penetrator. Beyond the constant subgrid in the x-y plane, an expansion factor of 1.1 was used to keep problem size and runtime within practical limits. In the z-direction, or axial direction, a constant cell spacing was used, which was 1.5 times the spacing of the constant subgrid in the x-y plane. The number of cells used to model a particular problem depended on the size of the target plates and overall length of the penetrator; however, the cell sizes in the constant sub-grid remained the same for all simulations. Appendix A contains a listing of KEEL input data for all of the problems modeled. If the only difference in a particular problem was the striking velocity, input data is listed for only one velocity.

The hydrodynamic behavior of the metals were modeled using the Mie-Gruneisen equation of state. The coefficients for the equation of state data were obtained from Kohn[13].

An incremental elastic-plastic formulation following the description given by Wilkins[14] is used to describe the deviatoric response of the metals. An elastic-perfectly plastic model has been used for the tungsten alloy and RHA with

20 kb[15] and 15 kb[15] yield strengths, respectively. A complete listing of the material properties and equation of state data are provided in Appendix B.

3. RESULTS AND DISCUSSION

Residual penetrator mass and residual kinetic energy have been used to measure performance. The greater the residual penetrator mass at a given velocity, the greater its performance. Residual mass was determined using the same technique ballisticians use to determine residual mass from radiographs. The complete set of density contour plots from which residual mass was determined can be found in Appendix C. Residual kinetic energy was determined using the residual mass from density contour plots and the velocity from velocity histograms. For the segmented penetrators residual energy is the summation of the individual segment residuals.

Results for the simulations against the RHA spaced plates for T/D of 2 are summarized in Table 2. Table 2 shows a significantly greater (31 percent) residual mass for the monolithic penetrator at a velocity of 1.5 km/s. The residual kinetic energy of both monolithic and segmented penetrators are about the same. At higher striking velocities the segmented penetrator shows essentially the same if not greater performance than the monolithic penetrator. Figures 1 to 5 show velocity histograms and density contour plots for the segmented penetrator at a velocity of 1.5 km/s at various times. The figures show a sequence of events in which individual segments collide and eventually become misaligned, i.e. not colinear. At 2 km/s collisions between individual segments still occur. Figures 6 to 8 show the lead segment losing velocity after perforating the first target allowing the next segment the catch up. However, misalignment of individual segments is not observed. The collisions tend to make the segmented rod appear much like a monolithic rod since the lead segment is not entirely eroded before being impacted by a subsequent segment. At 4 km/s, see Figures 9 and 10, most of the lead segment is eroded in perforating the first target plate. Though the lead segment is impacted by the second segment, only minimal loss of kinetic energy takes place in the second segment. Trailing segments uninvolved in collision retain their initial velocities and suffer no loss in kinetic energy. Due to the decrease in the time interval between target plates, no further collisions occur until lead segments impact the next plate.

TABLE 2. Residual Mass of Monolithic and Segmented Rods (N=5, S/D=1) against T/D=2 Spaced Plates

Striking Velocity (km/s)	Striking Energy (MJ)	Segmented Residual Mass (gms)	Segmented Residual Energy (MJ)	Monolithic Residual Mass (gms)	Monolithic Residual Energy (MJ)
1.5	0.308	47.9	0.016	63.0	0.018
2.0	0.548	107.0	0.166	108.0	0.147
3.0	1.233	149.0	0.637	143.0	0.589
4.0	2.192	152.0	1.183	150.0	1.141

Results for the simulations against the RHA spaced plates for T/D of 4 are summarized in Table 3. Simulations at a velocity of 1.5 km/s were conducted, however, both the monolithic and segmented penetrators failed to perforate the second target plate and are therefore not included. Table 3 shows higher residual mass for the segmented penetrator at all striking velocities. The data presented in Table 3 shows the greater the striking velocity, the greater the increase in residual mass. Figures 11 and 12 show velocity histograms and contour plots for the segmented penetrator at a velocity of 2.0 km/s. As with the simulation for the T/D of 2 case at a velocity of 1.5 km/s, individual

segment interactions occur which lead to the misalignment of segments. At 3 km/s, more of the lead segment is eroded before any interaction occurs, see Figure 13. In Figure 13, what appears to be a single segment is a fraction of the preceding segment and the subsequent segment. The alignment of the segments is less severely affected, see Figure 14. Segment interactions are also observed well after perforation of the second target plate, leading to severe misalignment of the segments, see Figure 15. At 4 km/s the lead segment is almost entirely eroded before interactions occur, see Figure 16. In Figure 16, what appears to be a single lead segment is the almost entirely eroded second segment being impacted by the third segment.

TABLE 3. Residual Mass of Monolithic and Segmented Rods (N=5, S/D=1) against T/D=4 Spaced Plates

Striking Velocity (km/s)	Striking Energy (MJ)	Segmented Residual Mass (gms)	Segmented Residual Energy (MJ)	Monolithic Residual Mass (gms)	Monolithic Residual Energy (MJ)
2.0	0.548	18.4	0.0018	14.6	0.0003
3.0	1.233	68.6	0.250	58.1	0.186
4.0	2.192	99.9	0.725	62.0	0.413

The interactions between segments for both T/D of 2 and 4, suggest a spacing of 1 D is not optimum. The effect of segment spacing on performance for the T/D of 4 target has been studied numerically for segment spacing-to- penetrator diameter ratios, S/D, of 4 and 8. No segment interactions occurred in perforating the spaced plate array. However, the two lead segments for the S/D of 4 case collided well after (t=100 micro-seconds) perforating the second plate. This occurs because the lead segment did not completely erode during perforation of the second spaced plate. Thus the lead segment loses velocity allowing remaining segments to catch up. Table 4 shows the affect of segment spacing on penetrator performance. Note that as S/D increases the residual penetrator mass increases.

TABLE 4. Residual Mass vs Segment Spacing for Vs = 4.0 km/s, N = 5, and T/D = 4 Plates

Spacing Diameter	Residual Mass (gms)	Residual Energy (MJ)
none	62.0	0.413
1	99.0	0.725
4	108.0	0.864
8	126.0	0.985
1*	129.0	1.183

* 20 Segment Rod

Table 4 also presents the results for a 20 segment projectile with a S/D of 1. These results suggest that trailing segments, unaffected by impact with the spaced plates and/or individual segment interactions, retain more kinetic energy than an equivalent monolithic rod. Figures 17 and 18 show velocity histograms and density contour plots of the 20 segment penetrator and the equivalent monolithic penetrator. The monolithic penetrator's velocity is

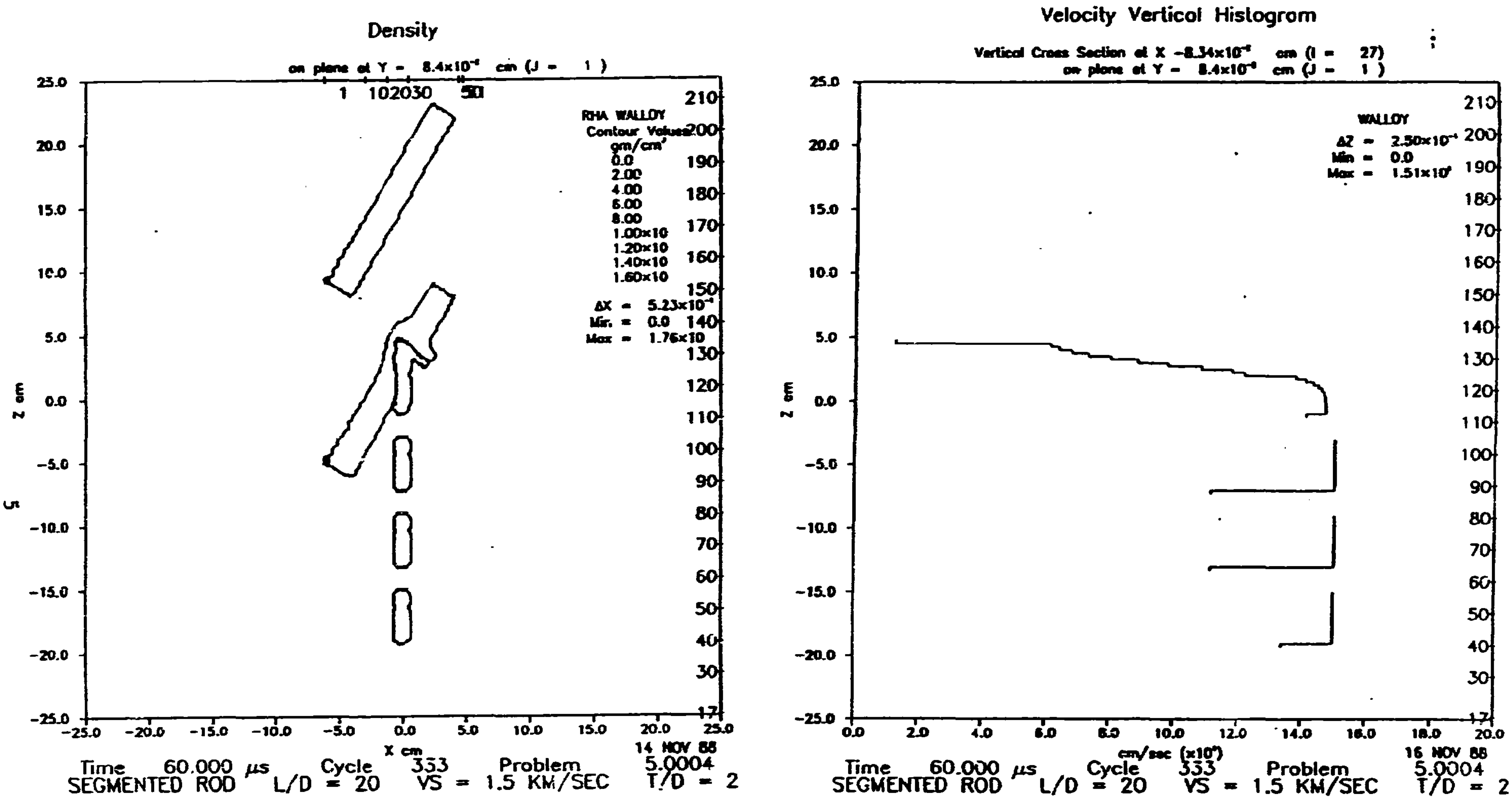

Figure 1. Segmented penetrator, N=5, V=1.5 km/s into 60° RHA (T/D=2) at 60 micro-seconds

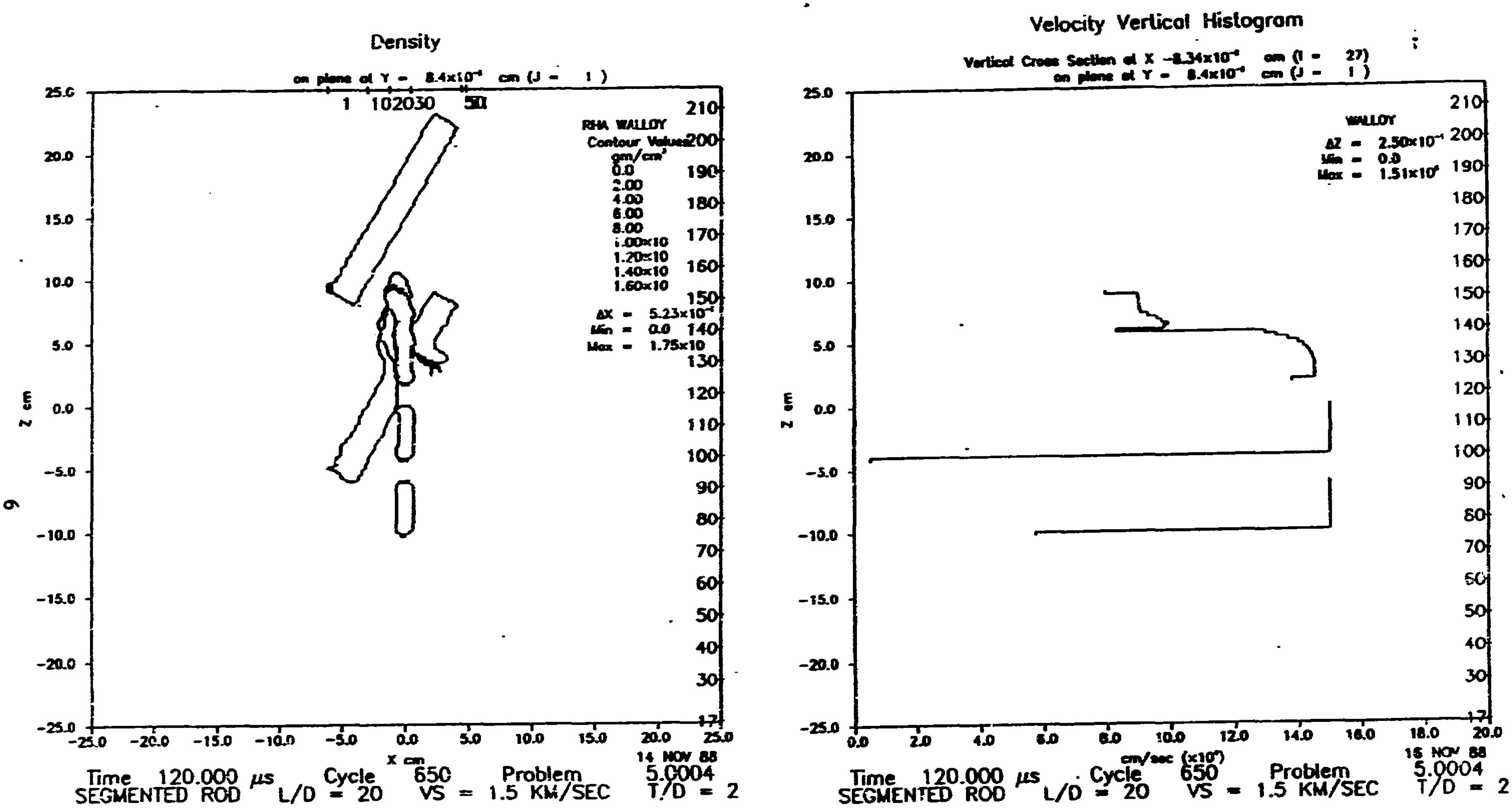

Figure 2. Segmented penetrator, N=5, V=1.5 km/s into 60° RHA (T/D=2) at 120 micro-seconds

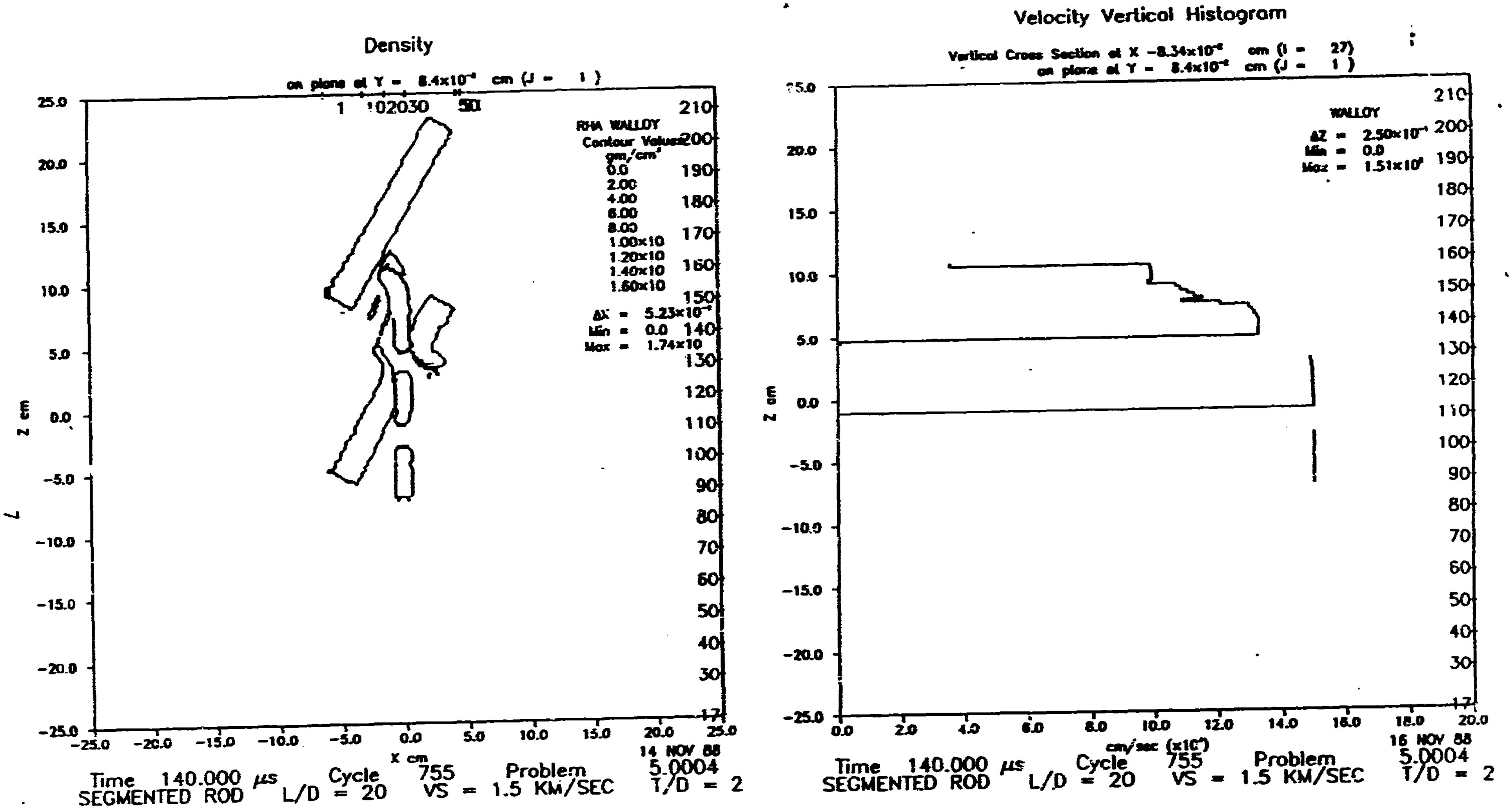

Figure 3. Segmented penetrator, N=5, V=1.5 km/s intc 60° RHA (T/D=2) at 140 micro-seconds

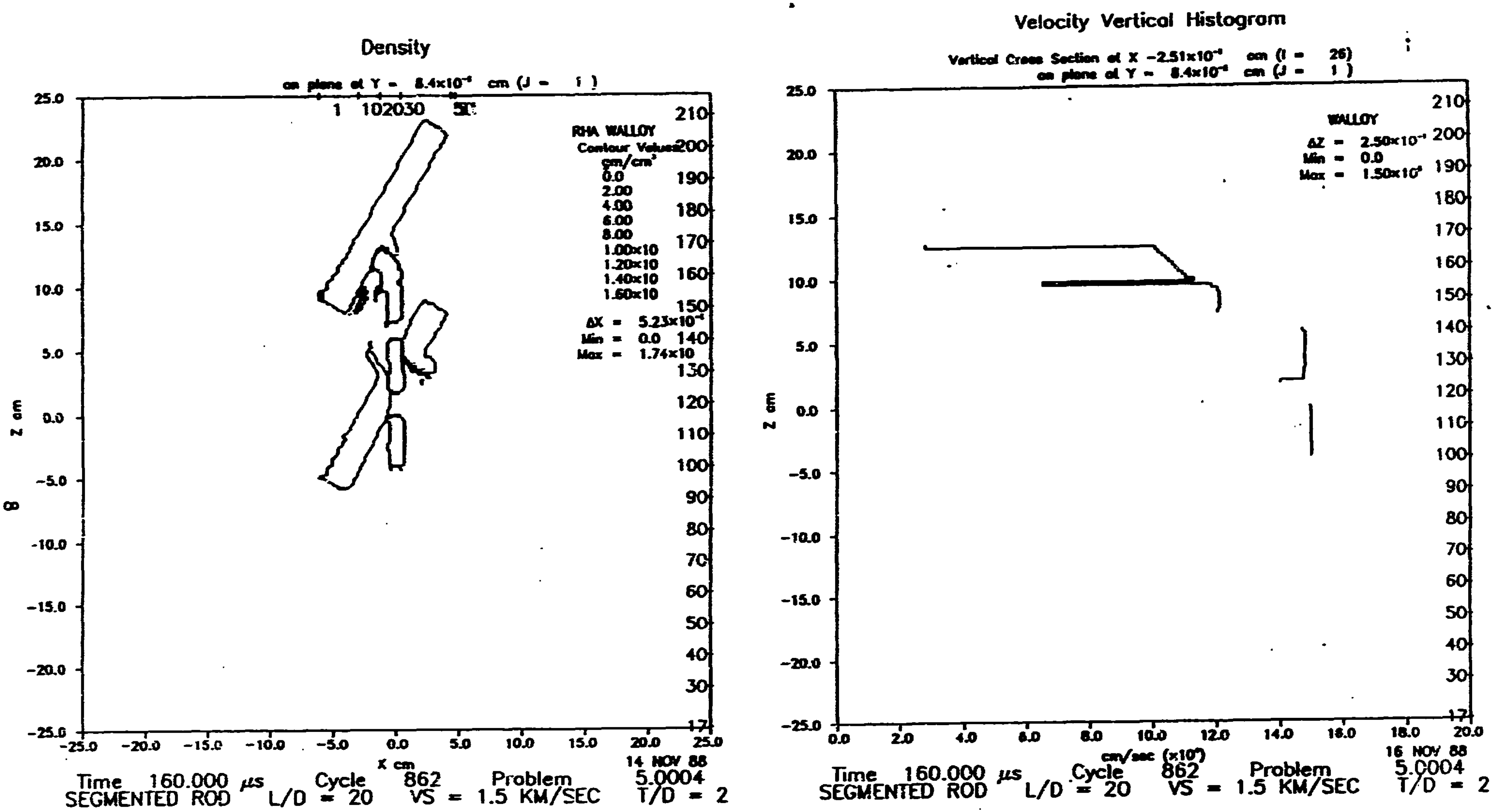

Figure 4. Segmented penetrator, N=5, V=1.5 km/s into 60° RHA (T/D=2) at 160 micro-seconds

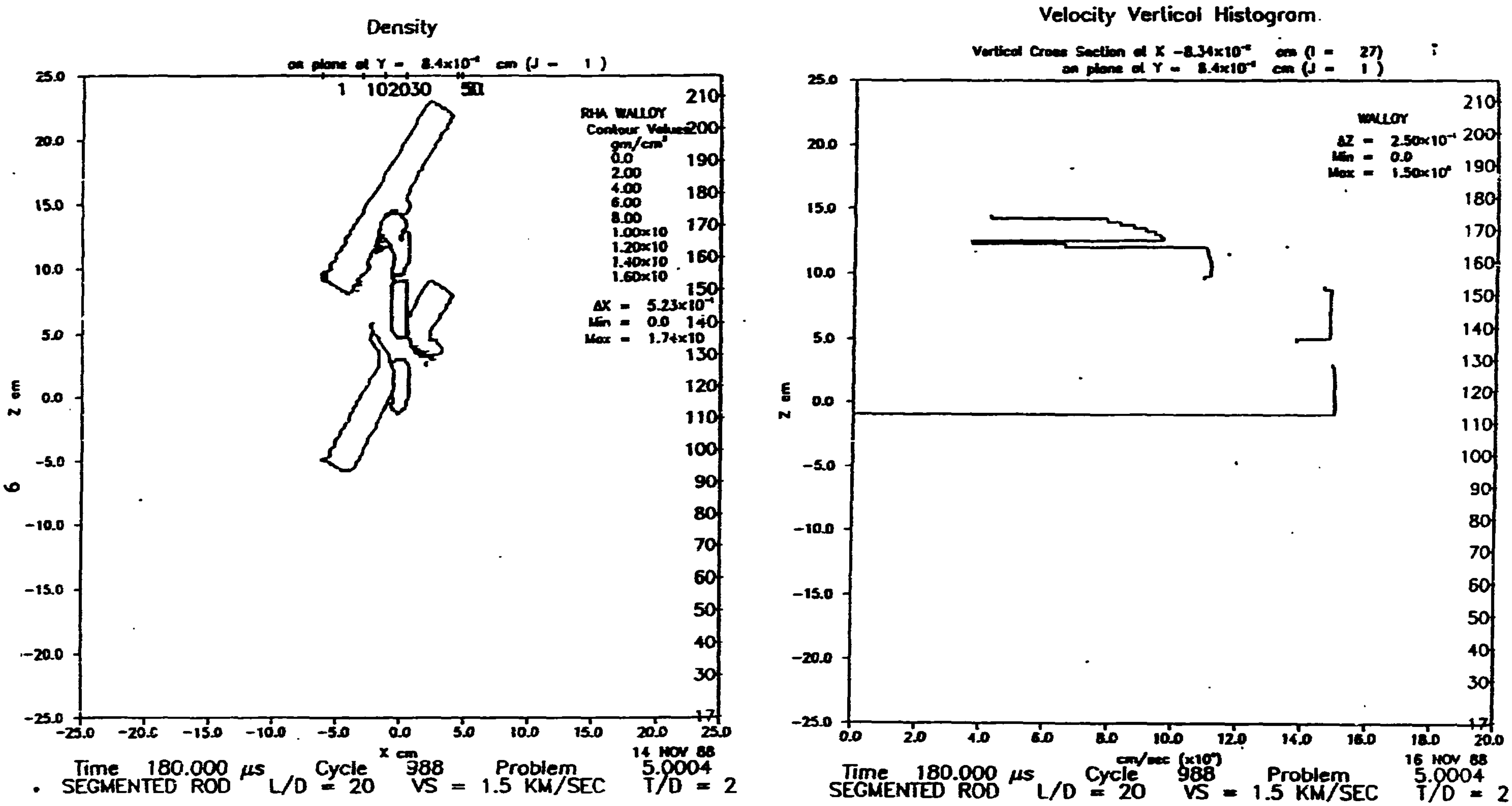

Figure 5. Segmented penetrator, N=5, V=1.5 km/s into 60° RHA (T/D=2) at 180 micro-seconds

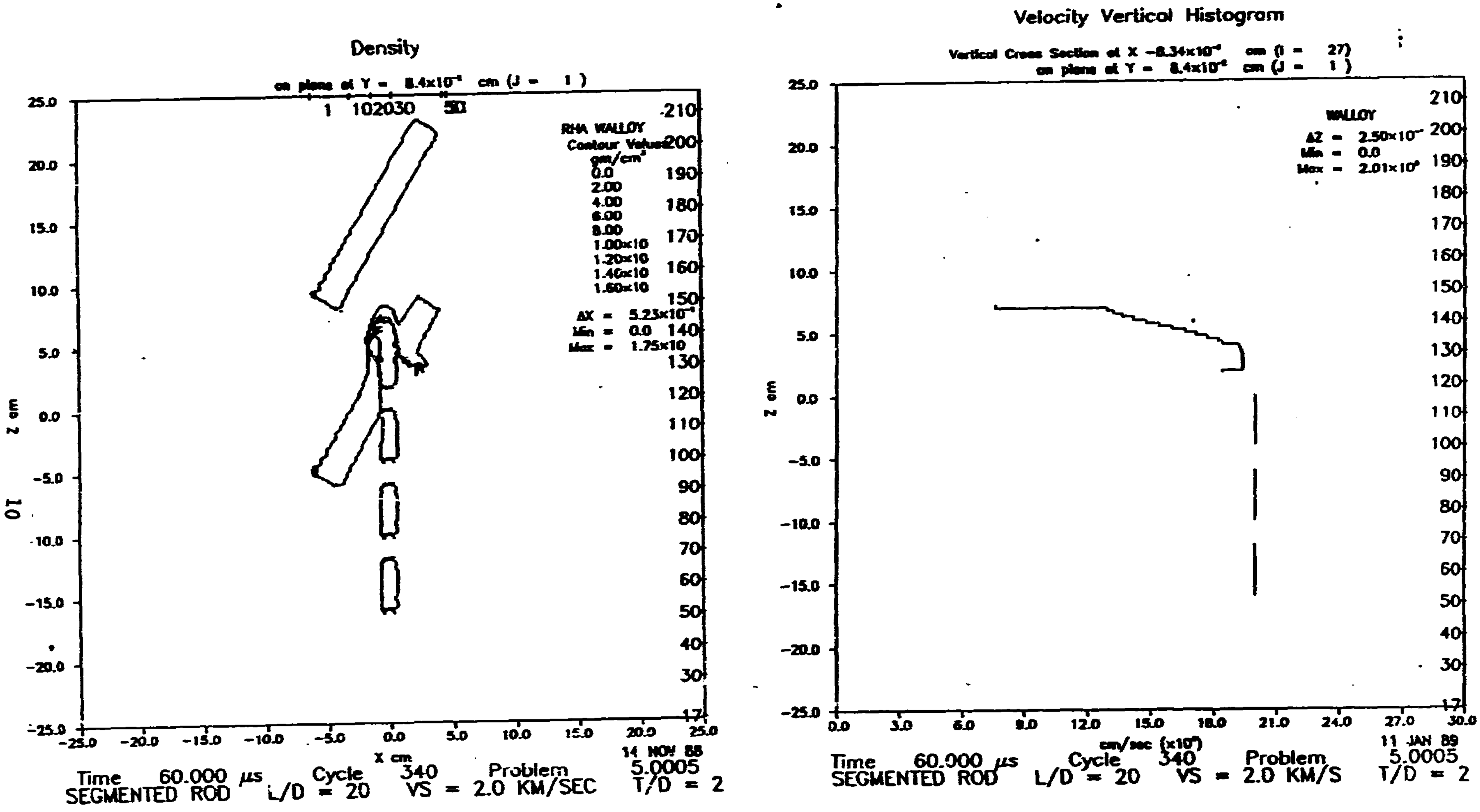

Figure 6. Segmented penetrator, N=5, V=2.0 km/s into 60° RHA (T/D=2) at 60 micro-seconds

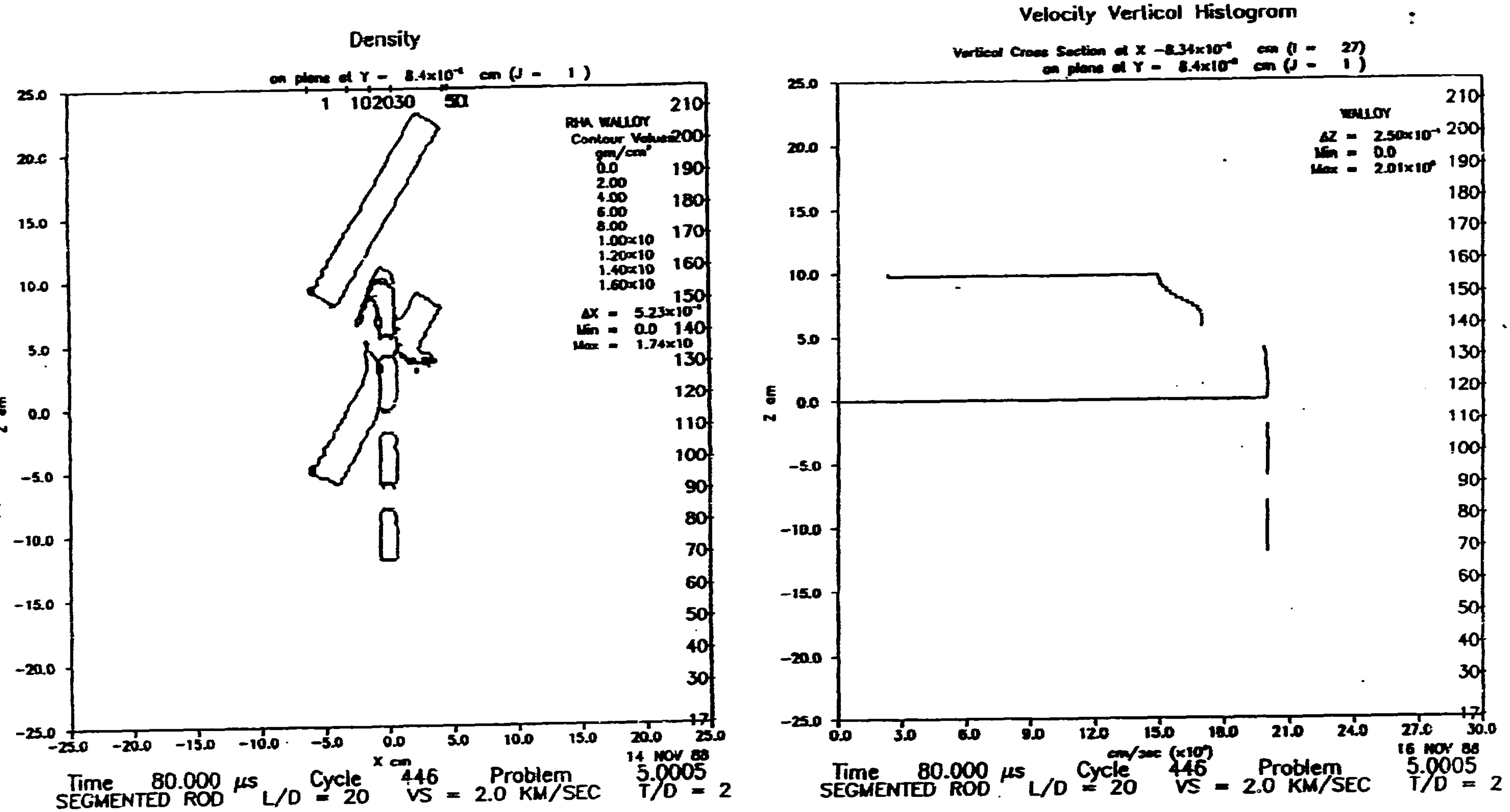

Figure 7. Segmented penetrator, N=5, V=2.0 km/s into 60° RHA (T/D=2) at 80 micro-seconds

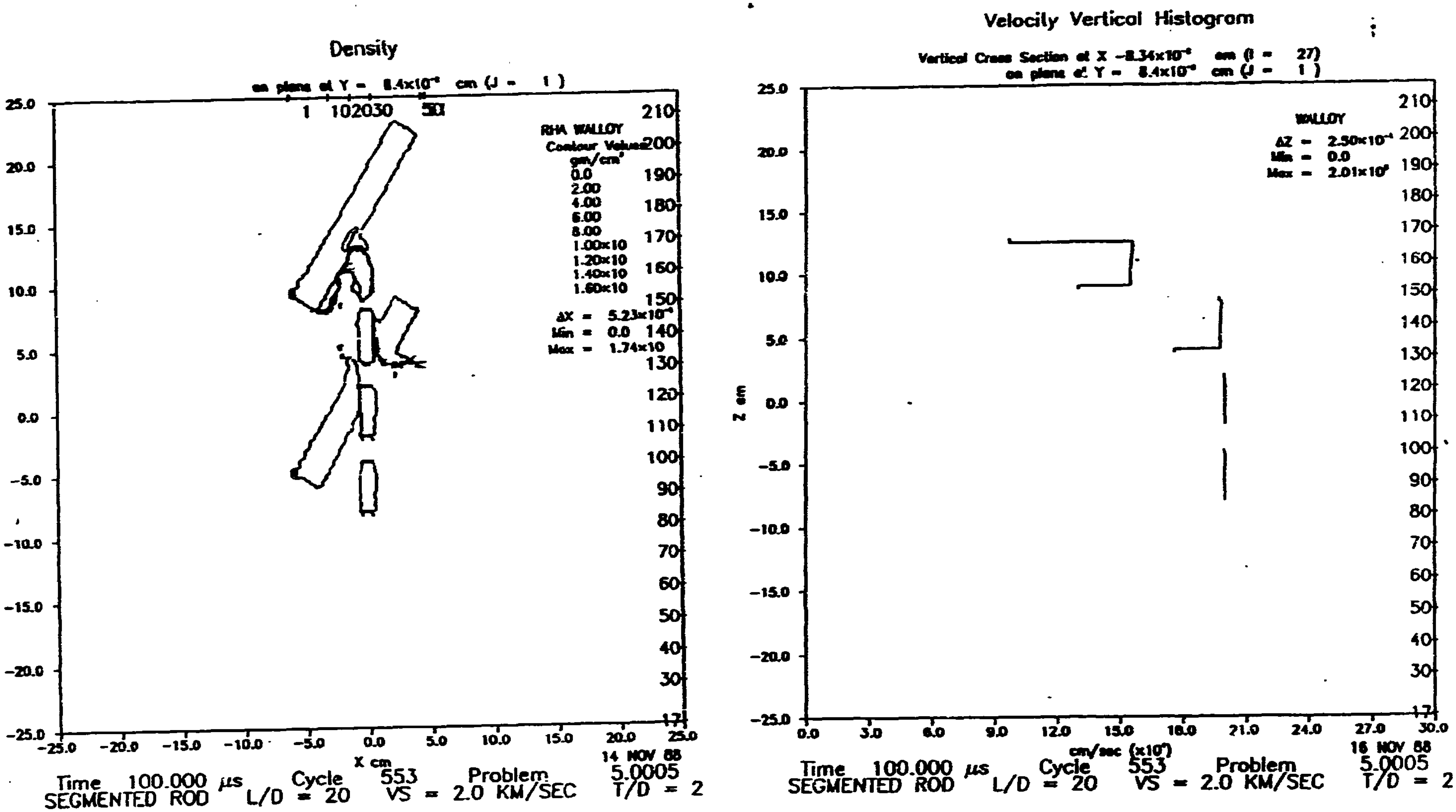

Figure 8. Segmented penetrator, N=5, V=2.0 km/s into 60° RHA (T/D=2) at 100 micro-seconds

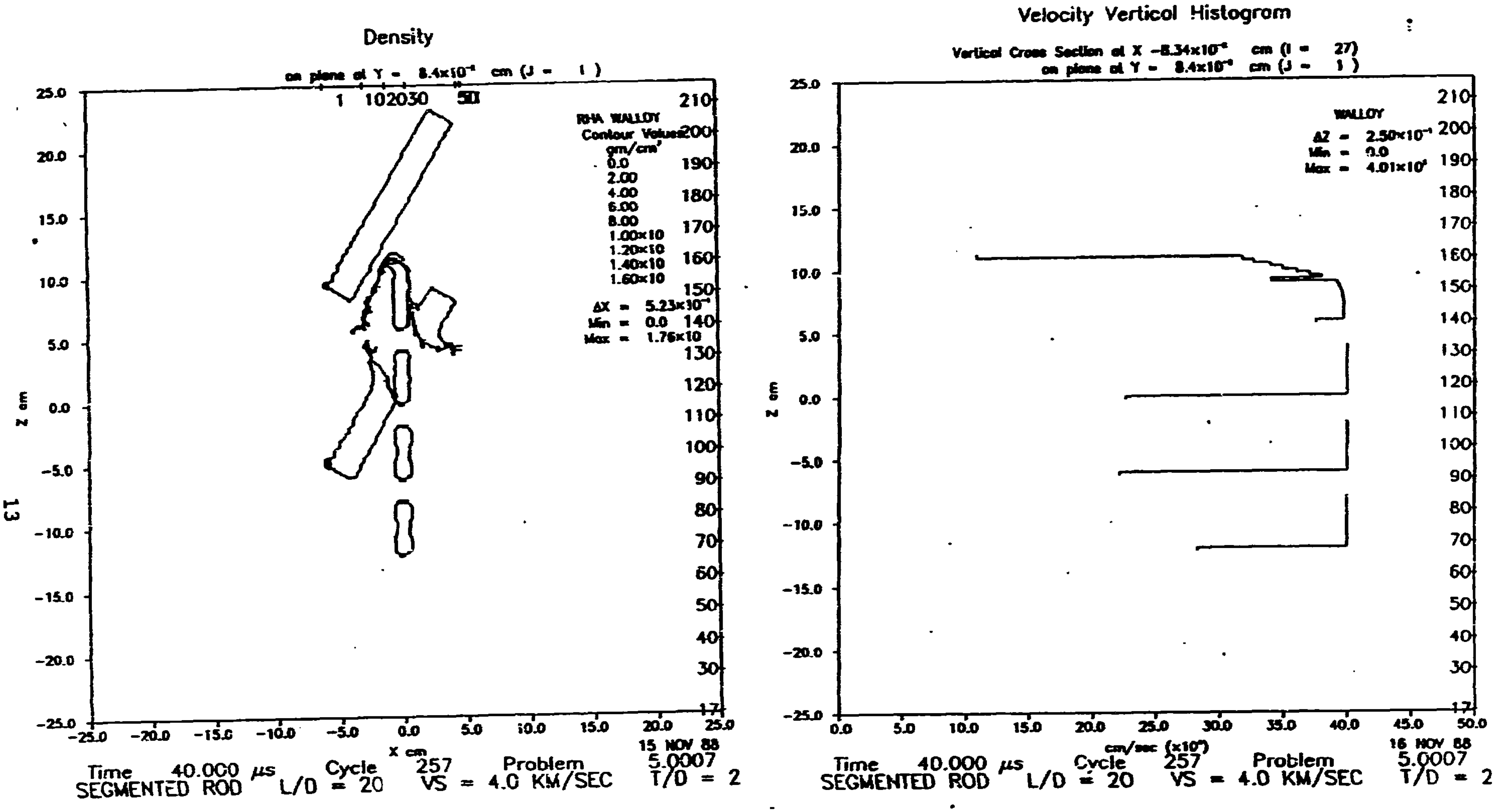

Figure 9. Segmented penetrator, N=5, V=4.0 km/s into 60° RHA (T/D=2) at 40 micro-seconds

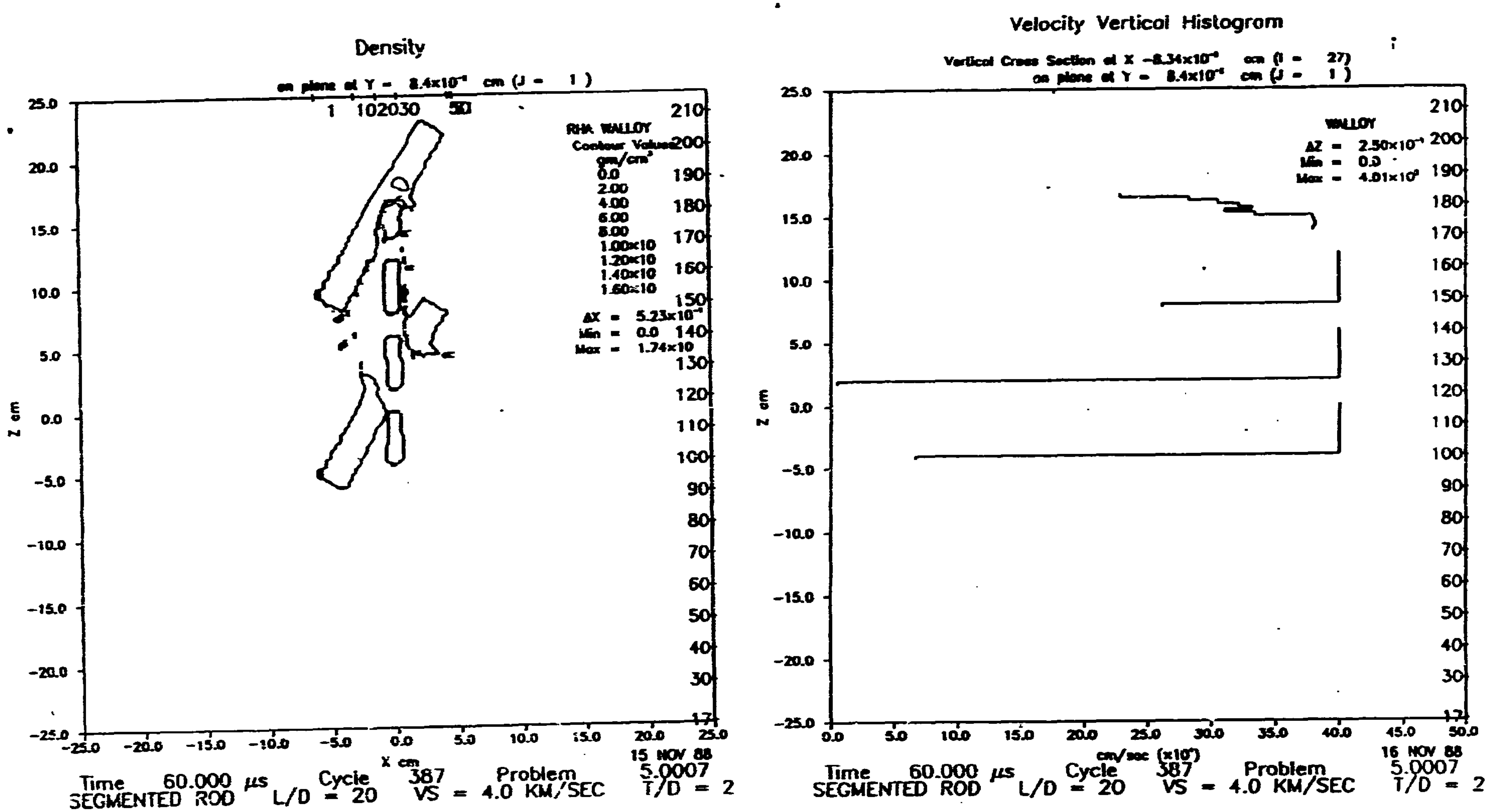

Figure 10. Segmented penetrator, N=5, V=4.0 km/s into 60° RHA (T/D=2) at 60 micro-seconds

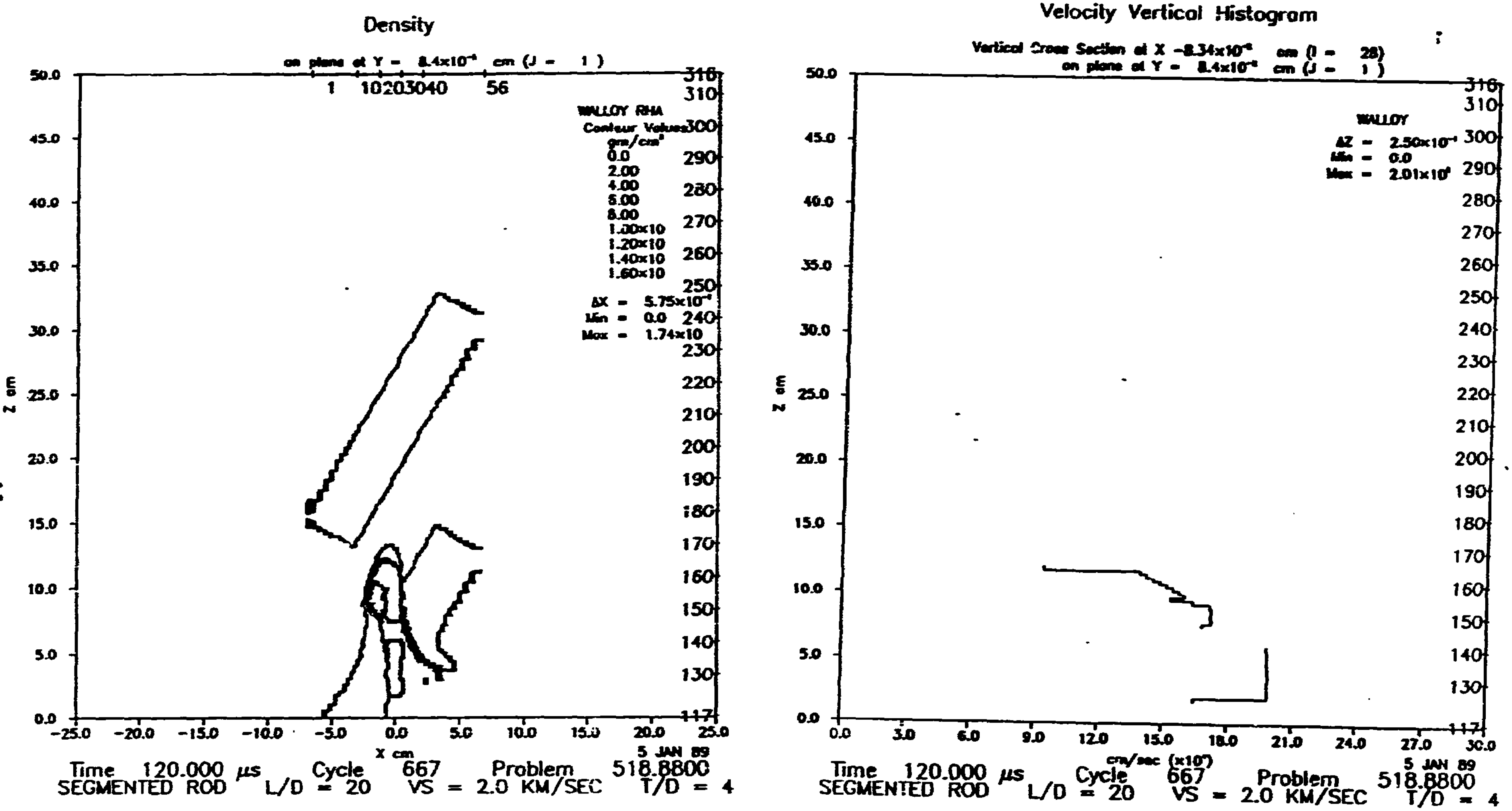

Figure 11. Segmented penetrator, N=5, V=2.0 km/s into 60° RHA (T/D=4) at 120 micro-seconds

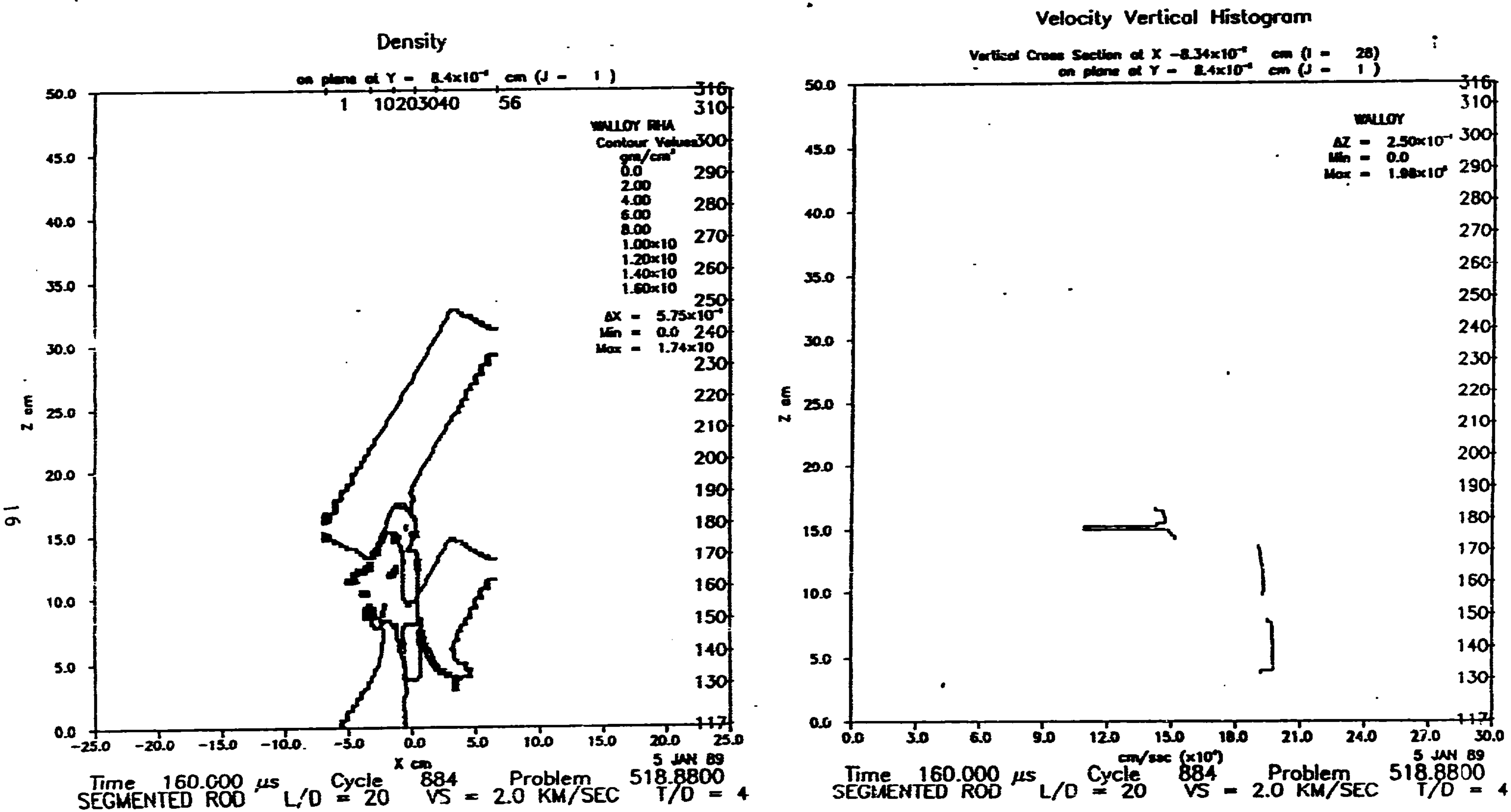

Figure 12. Segmented penetrator, N=5, V=2.0 km/s into 60° RHA (T/D=4) at 160 micro-seconds

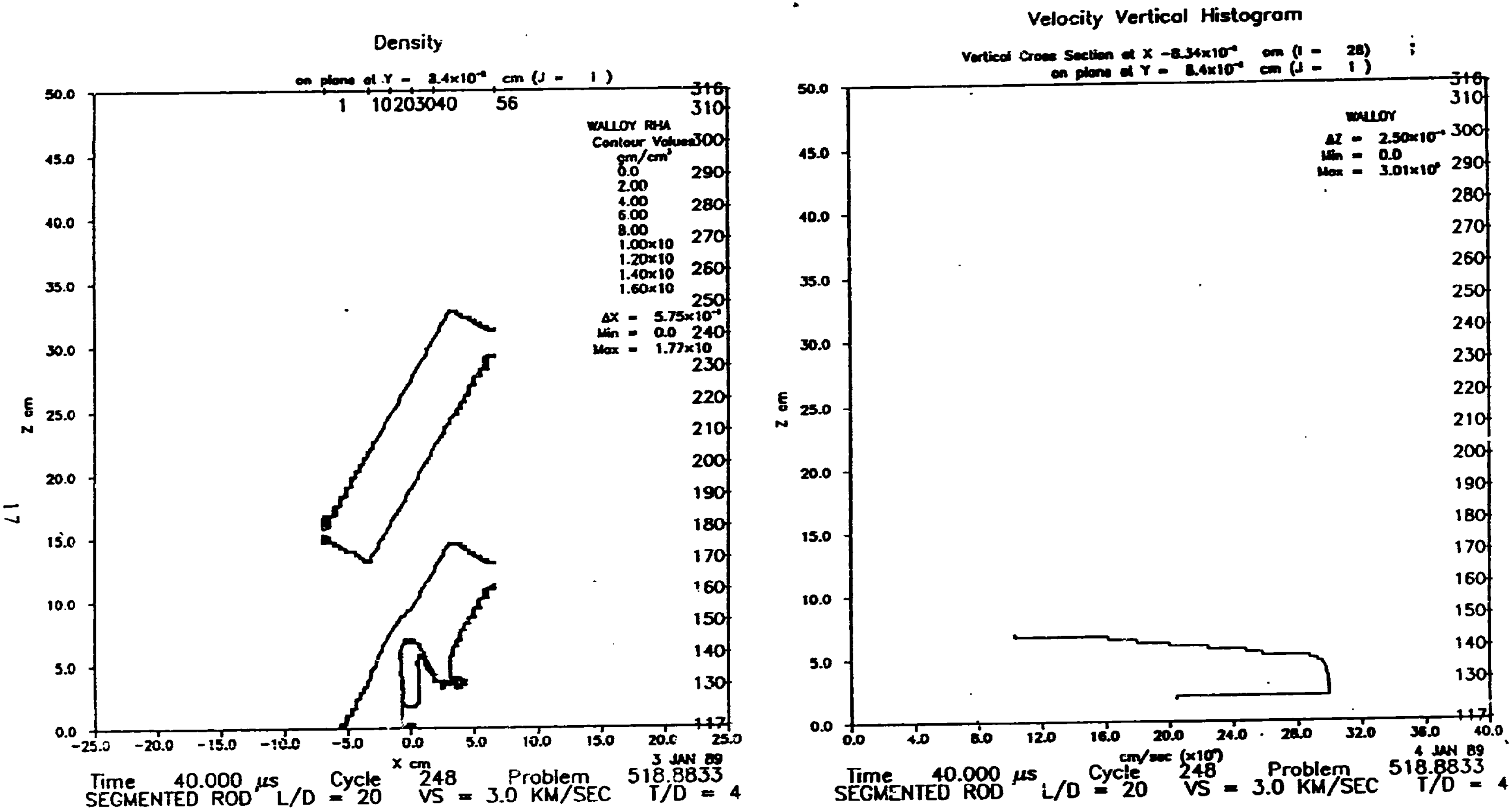

Figure 13. Segmented penetrator, N=5, V=3.0 km/s into 60° RHA (T/D=4) at 40 micro-seconds

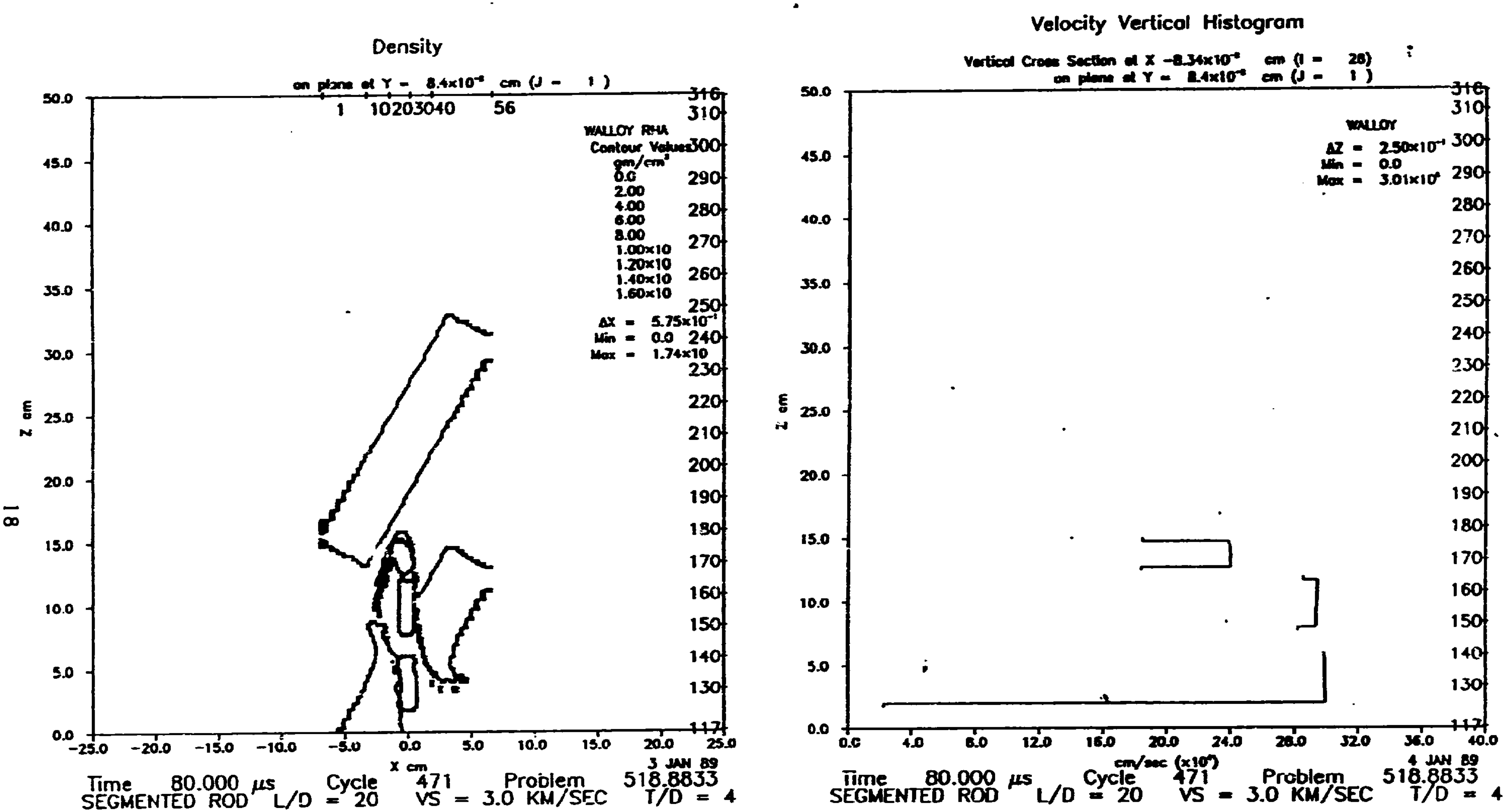

Figure 14. Segmented penetrator, N=5, V=3.0 km/s into 60° RHA (T/D=4) at 80 micro-seconds

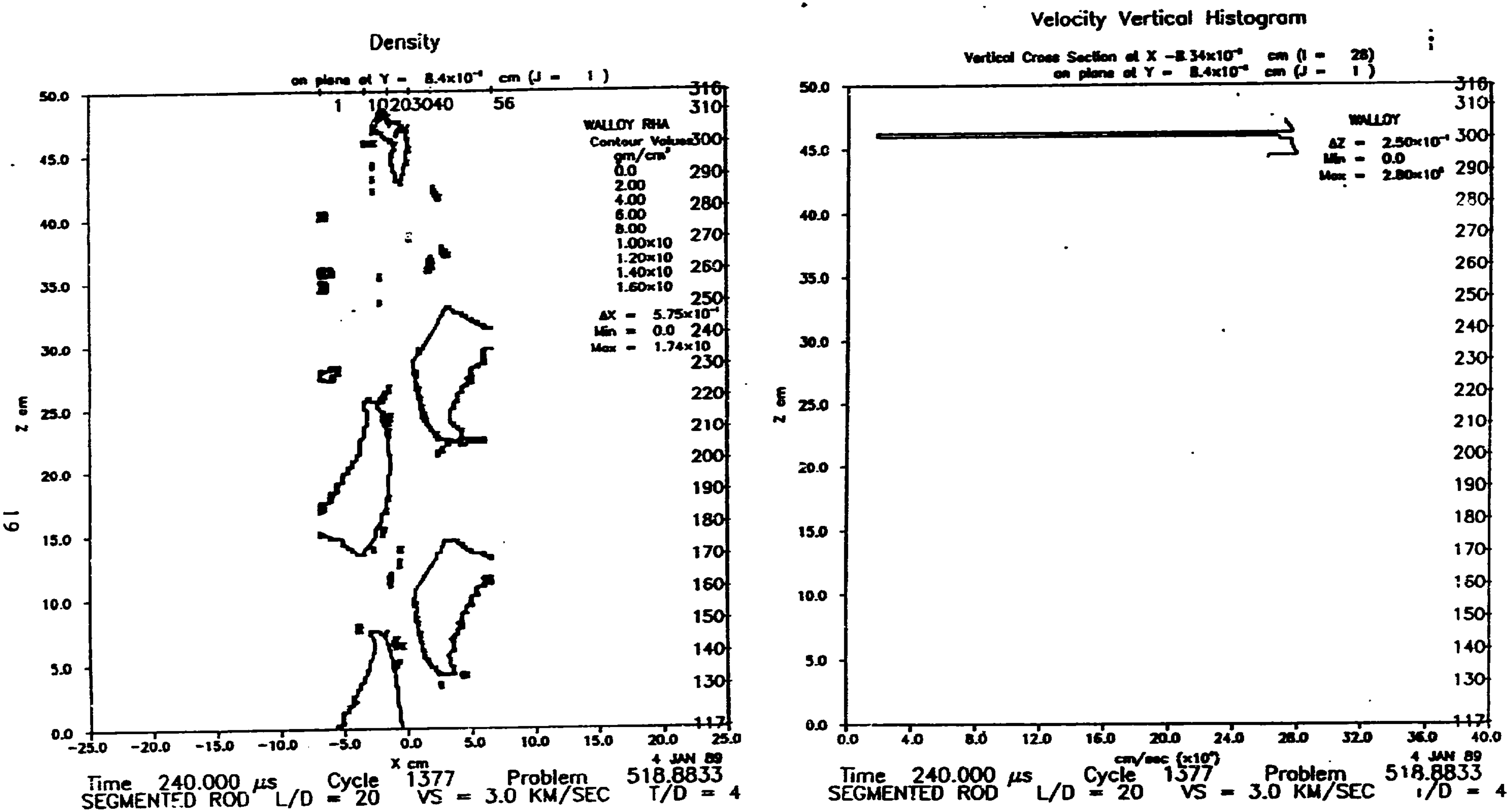

Figure 15. Segmented penetrator, N=5, V=3.0 km/s into 60° RHA (T/D=4) at 240 micro-seconds

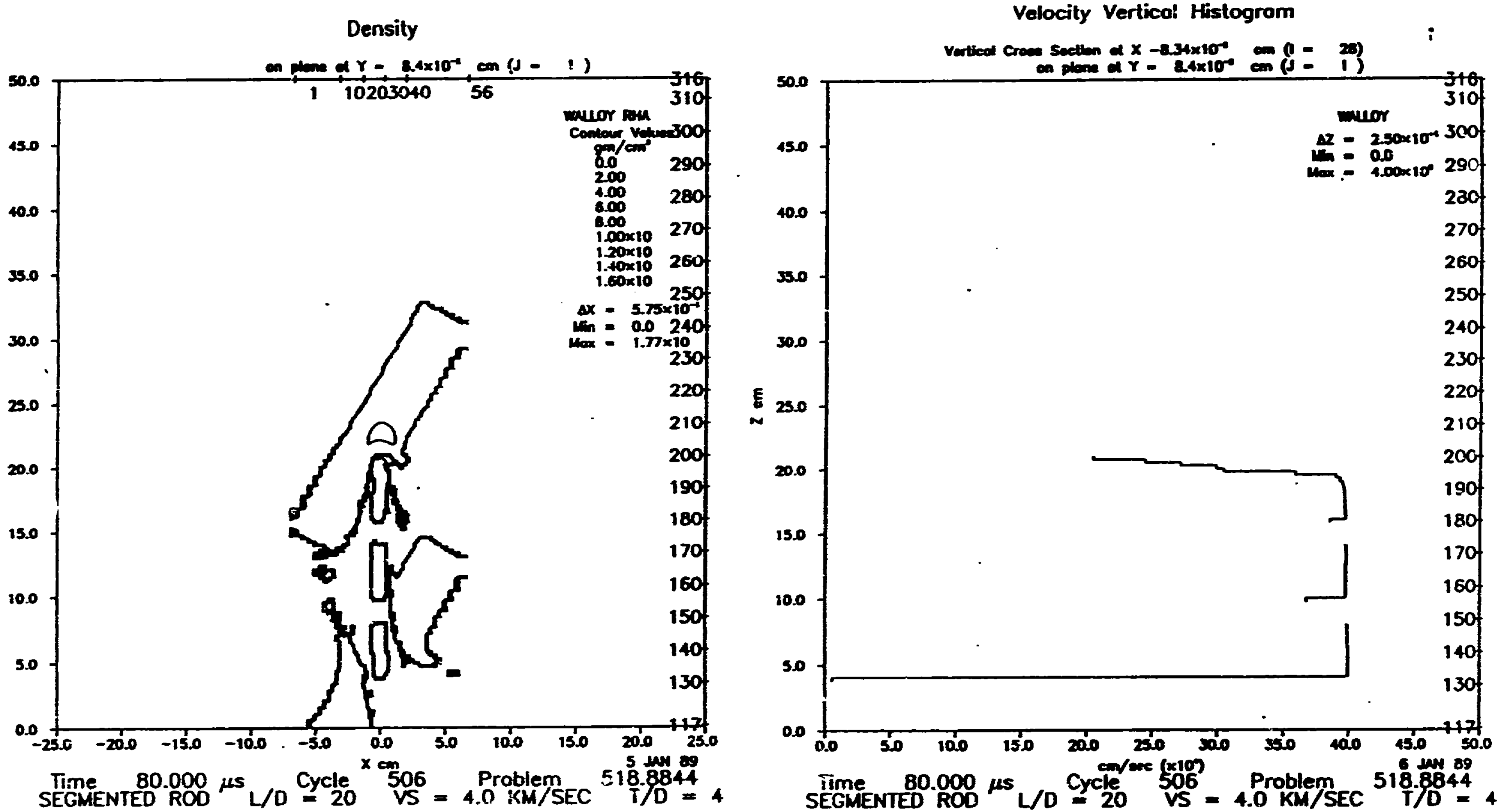

Figure 16. Segmented penetrator, N=5, V=4.0 km/s into 60° RHA (T/D=4) at 120 micro-seconds

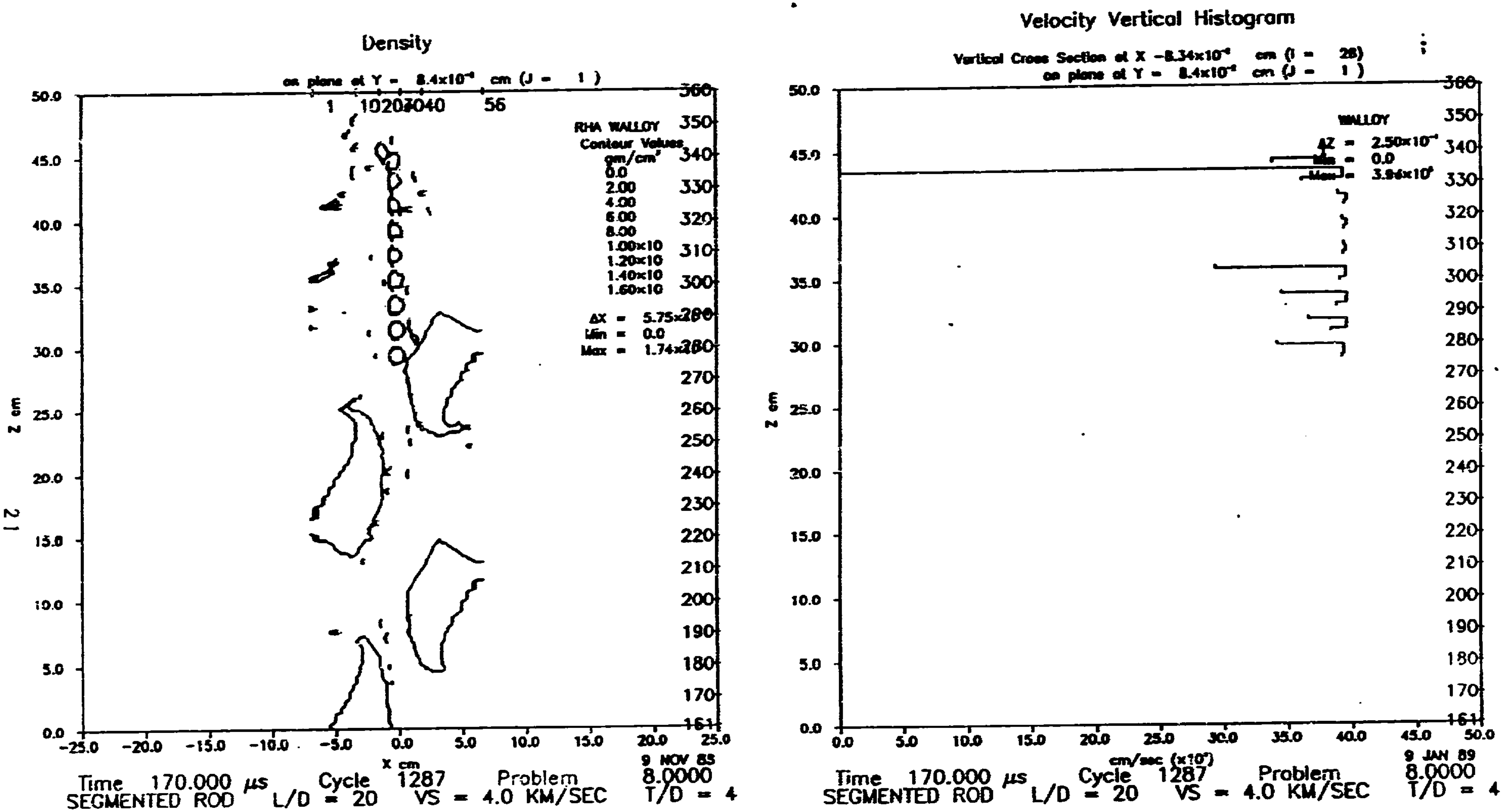

Figure 17. Segmented penetrator, N=20, V=4.0 km/s into 60° RHA (T/D=4) at 170 micro-seconds

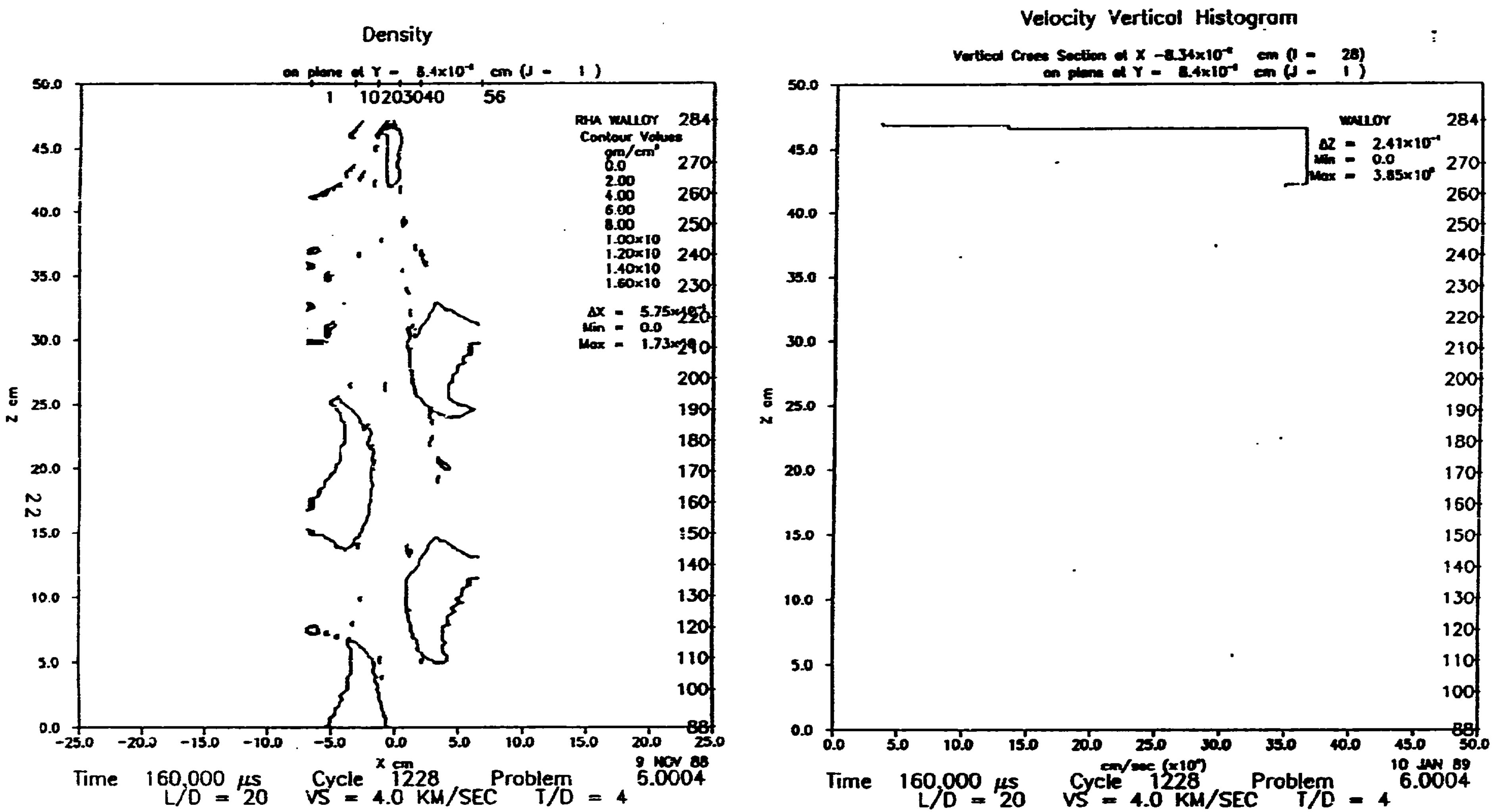

Figure 18. Monolithic penetrator, N=1, V=4.0 km/s into 60° RHA (T/D=4) at 160 micro-seconds

reduced while perforating the spaced plate array, while trailing segments unaffected by interactions retain their initial striking velocity. Table 4 shows a 108 percent improvement in residual mass over the equivalent monolithic rod. The improvement in residual mass of the 5 segment penetrator with an S/D of 8 over the equivalent monolithic rod is 103 percent.

4. CONCLUSIONS

A number of 3-D simulations have been conducted to determine the performance of segmented rods impacting spaced plate arrays. The performance of segmented rods is characterized based on residual mass and kinetic energy. In general, segmented rods outperform their monolithic counterparts for the spaced plate arrays studied at velocities above 2 km/s. The increase in performance is enhanced for thick target plates. Furthermore, the simulations show that increasing the spacing between segments increases performance. It is desirable, though not always practical, for spacing to be such that every segment acts as an independent penetrator. Finally, it should be noted that increasing the number of segments increases the residual mass and kinetic energy. The increase in performance derived from a greater number of segments is greater than the increase derived from increased segment spacing.

LIST OF REFERENCES

1. Kucher, V. "Multiple Impacts on Monolithic Steel", Ballistic Research Laboratory Technical Report ARBRL-TR-02406, April 1982.

2. de Rosset, W. S. and Kimsey, K. D., "Calculation of Multiple Copper Rod Impacts on Steel Targets", Proc. Ninth International Symposium on Ballistics, Shrivenham, U. K., April 29-30, May 1, 1986.

3. Scheffler, D. R.,"2-D Computer Simulations of Segmented Penetrators", Ballistic Research Laboratory Technical Report, BRL-TR-3013, July 1989.

4. Sedgwick, R. T., Waddell, J. L., and Wilkinson, G. M., "High Velocity Long Rod Impact: Theory and Experiment", Proc. Tenth International Symposium on Ballistics, San Diego, October 1987.

5. Charters, A. C., "The Penetration of Rolled Homogenous Armor by Continuous and Segmented Rods at High Velocity: Theory and Experiments", General Research Corporation Technical Report CR-86-1031, April 1986.

6. Charters, A. C., "The Penetration of Rolled Homogenous Armor by Continuous and Segmented Rods at High Velocity: Theory and Experiments", General Research Corporation Technical Report CR-87-1008, December 1986.

7. Charters, A. C., and Menna, T. L., "Armor/Anti-armor Program: Advanced Penetrator Concepts Evaluation Program", General Research Corporation briefing package presented at the DARPA Armor/Anti-Armor Executive Steering Committee, Arlington, Virginia, August 25, 1987.

8. Charters, A. C., and Menna, T. L., "Armor/Anti-armor Program: Second Quarterly Review", General Research Corporation briefing package presented at the DARPA Impact Physics Team Second Quarterly Review, Lawrence Livermore National Laboratories, October 14-15, 1987.

9. Bell, L. P., "Evaluation of Segmented and Solid Projectiles During Hypervelocity Flight and Impact", Arnold Engineering Development Center Technical Report AEDC-TRS-87-V6, March 1987.

10. Matuska, D. A. and Osborn, J. J.,"HULL Technical Manual", vol I, Orlando Technology Incorporated, 1986.

11. Matuska, D. A. and Osborn, J. J.,"HULL Users Manual", vol II, Orlando Technology Incorporated, 1986.

12. Hancock, J. W., and Mackenzie, A. C., J. Mech. Phys. Solids, 24, 147.

13. Kohn, B. J., "Compilation of Hugoniot Equations of State", Air Force Weapons Laboratory Technical Report AFWL-TR-69-38, April 1969.

14. Wilkins, M. L., in B. Adler et al. (Eds.), Methods in Computational Physics, Academic Press, New York, 1964.

15. Nicholas, T., "Dynamic Tensile Testing of Structural Materials Using a Split Hopkinson Bar Apparatus", Air Force Wright Aeronautical Laboratories Technical Report AFWAL-TR-80-4053, October 1980.

APPENDIX A - KEEL Input Data

```
KEEL PROBLEM 5.0000
NM=3 AIR=1 WALLOY=2 RHA=3
DIMEN=3 VISC=1 FLUXER=3 STRESS=1
IMAX=51 JMAX=31 KMAX=241 IQ=50 JQ=30 KQ=240
FAIL=1 STRAIN=1 REZONE=0
NSTN=2 NOP=2000
AREF=.TRUE. BREF=.FALSE. FREF=.FALSE.
LREF=.FALSE. RREF=.FALSE. TREF=.FALSE.
HEADER
 L/D = 20  VS = 1.5 KM/SEC  T/D = 2
MESH
CONSTANT SUBGRID  NX=30 X0=-2.5 XMAX=2.5 RXNEG=1.1 RXPOS=1.1
                X0LIM=-6.42045 XMLIM=4.98957
                NY=15 Y0=0.0 YMAX=2.5 RYPOS=1.1
                Y0LIM=0. YMLIM=9.09078
                NZ=241 Z0=-21.0 ZMAX=39.25 RZNEG=1.0
                                RZPOS=1.0
                Z0LIM=-21.0 ZMLIM=39.25
GENERATE
 PACKAGE WALLOY W=1.5E5
  CYLINDER XC=0.0 YC=0.0 ZB=-20. ZT=-0.0 RADIUS=.5
 PACKAGE AIR W=1.5E5
  CYLINDER XC=0.0 YC=0.0 ZB=-1.0E20 ZT=-20. RADIUS=.5
 PACKAGE RHA
  BOX X1=-8.0 X2=8.0 Y1=0.0 Y2=8.0 Z1=0.0 Z2=2.0
  XCC=0.0 YCC=0.0 ZCC=0.86603
  ANGLB=60
 PACKAGE RHA
  BOX X1=-8.0 X2=8.0 Y1=0.0 Y2=8.0 Z1=0.0 Z2=2.0
  XCC=0.0 YCC=0.0 ZCC=15.02603
  ANGLB=60
 PACKAGE AIR W=1.0E4 BOX FILL
  STATION XS=0. YS=0. ZL=0.
       XS=0. YS=0. ZL=-20.
END
```

```
KEEL PROBLEM 5.0004
NM=3 AIR=1 WALLOY=2 RHA=3
DIMEN=3 VISC=1 FLUXER=3 STRESS=1
IMAX=51 JMAX=31 KMAX=273 IQ=50 JQ=30 KQ=272
FAIL=1 STRAIN=1 REZONE=0
NSTN=2 NOP=2000
AREF=.TRUE. BREF=.FALSE. FREF=.FALSE.
LREF=.FALSE. RREF=.FALSE. TREF=.FALSE.
HEADER
 L/D = 20  VS = 1.5 KM/S  T/D = 2
MESH
CONSTANT SUBGRID  NX=30 X0=-2.5 XMAX=2.5 RXNEG=1.1 RXPOS=1.1
                  X0LIM=-6.42045 XMLIM=4.98957
                  NY=15 Y0=0.0 YMAX=2.5 RYPOS=1.1
                  Y0LIM=0. YMLIM=9.09078
                  NZ=273 Z0=-29.0 ZMAX=39.25 RZNEG=1.0
                                 RZPOS=1.0
                  Z0LIM=-29.0 ZMLIM=39.25
GENERATE
 PACKAGE WALLOY W=1.5E5
  CYLINDER XC=0.0 YC=0.0 ZB=-4. ZT=-0.0 RADIUS=.5
 PACKAGE AIR W=1.5E5
  CYLINDER XC=0.0 YC=0.0 ZB=-6. ZT=-4. RADIUS=.5
 PACKAGE WALLOY W=1.5E5
  CYLINDER XC=0.0 YC=0.0 ZB=-10. ZT=-6. RADIUS=.5
 PACKAGE AIR W=1.5E5
  CYLINDER XC=0.0 YC=0.0 ZB=-12. ZT=-10. RADIUS=.5
 PACKAGE WALLOY W=1.5E5
  CYLINDER XC=0.0 YC=0.0 ZB=-16. ZT=-12. RADIUS=.5
 PACKAGE AIR W=1.5E5
  CYLINDER XC=0.0 YC=0.0 ZB=-18. ZT=-16. RADIUS=.5
 PACKAGE WALLOY W=1.5E5
  CYLINDER XC=0.0 YC=0.0 ZB=-22. ZT=-18. RADIUS=.5
 PACKAGE AIR W=1.5E5
  CYLINDER XC=0.0 YC=0.0 ZB=-24. ZT=-22. RADIUS=.5
 PACKAGE WALLOY W=1.5E5
  CYLINDER XC=0.0 YC=0.0 ZB=-28. ZT=-24. RADIUS=.5
 PACKAGE AIR W=1.5E5
  CYLINDER XC=0.0 YC=0.0 ZB=-1.0E20 ZT=-28. RADIUS=.5
 PACKAGE RHA
  BOX X1=-8.0 X2=8.0 Y1=0.0 Y2=8.0 Z1=0.0 Z2=2.0
  XCC=0.0 YCC=0.0 ZCC=0.86603
  ANGLB=60
 PACKAGE RHA
  BOX X1=-8.0 X2=8.0 Y1=0.0 Y2=8.0 Z1=0.0 Z2=2.0
  XCC=0.0 YCC=0.0 ZCC=15.02603
  ANGLB=60
 PACKAGE AIR W=1.0E4 BOX FILL
  STATION XS=0. YS=0. ZL=0.
          XS=0. YS=0. ZL=-28.
END
```

```
KEEL PROBLEM 6.0001
NM=3 AIR=1 WALLOY=2 RHA=3
DIMEN=3 VISC=1 FLUXER=3 STRESS=1
IMAX=56 JMAX=33 KMAX=284 IQ=55 JQ=32 KQ=283
FAIL=1 STRAIN=1 REZONE=0
NSTN=2 NOP=2000
AREF=.TRUE. BREF=.FALSE. FREF=.FALSE.
LREF=.FALSE. RREF=.FALSE. TREF=.FALSE.
HEADER
 L/D = 20  VS = 1.5 KM/SEC  T/D = 4
MESH
CONSTANT SUBGRID  NX=30 X0=-2.5 XMAX=2.5 RXNEG=1.1 RXPOS=1.1
               X0LIM=-6.99583 XMLIM=6.99583
               NY=15 Y0=0.0 YMAX=2.5 RYPOS=1.1
               Y0LIM=0. YMLIM=10.85985
               NZ=296 Z0=-21.0 ZMAX=47.25 RZNEG=1.0
                          RZPOS=1.0
               Z0LIM=-21.0 ZMLIM=50.
GENERATE
 PACKAGE WALLOY W=1.5E5
  CYLINDER XC=0.0 YC=0.0 ZB=-20. ZT=-0.0 RADIUS=.5
 PACKAGE AIR W=1.5E5
  CYLINDER XC=0.0 YC=0.0 ZB=-1.0E20 ZT=-20. RADIUS=.5
 PACKAGE RHA
  BOX X1=-10.0 X2=10.0 Y1=0.0 Y2=10.0 Z1=0.0 Z2=4.0
  XCC=1.7321 YCC=0.0 ZCC=3.86603
  ANGLB=60
 PACKAGE RHA
  BOX X1=-10.0 X2=10.0 Y1=0.0 Y2=10.0 Z1=0.0 Z2=4.0
  XCC=1.7321 YCC=0.0 ZCC=22.02603
  ANGLB=60
 PACKAGE AIR W=1.0E4 BOX FILL
  STATION XS=0. YS=0. ZL=0.
      XS=0. YS=0. ZL=-20.
END
```

KEEL Input For Segmented Penetrators Into T/D=4 Spaced Plates

```
KEEL PROBLEM 518.88
NM=3 AIR=1 WALLOY=2 RHA=3
DIMEN=3 VISC=1 FLUXER=3 STRESS=1
IMAX=56 JMAX=33 KMAX=316 IQ=53 JQ=32 KQ=315
FAIL=1 STRAIN=1 REZONE=0
NSTN=2 NOP=2000
AREF=.TRUE. BREF=.FALSE. FREF=.FALSE.
LREF=.FALSE. RREF=.FALSE. TREF=.FALSE.
HEADER
 SEGMENTED ROD  L/D = 20  VS = 2.0 KM/SEC  T/D = 4
MESH
CONSTANT SUBGRID  NX=30 X0=-2.5 XMAX=2.5 RXNEG=1.1 RXPOS=1.1
             X0LIM=-6.99583 XMLIM=6.99583
             NY=15 Y0=0.0 YMAX=2.5 RYPOS=1.1
             Y0LIM=0. YMLIM=10.85985
             NZ=316 Z0=-29.0 ZMAX=50. RZNEG=1.0
                               RZPOS=1.0
             Z0LIM=-29.0 ZMLIM=50.
GENERATE
 PACKAGE WALLOY W=2.0E5
  CYLINDER XC=0.0 YC=0.0 ZB=-4. ZT=-0.0 RADIUS=.5
 PACKAGE AIR W=2.0E5
  CYLINDER XC=0.0 YC=0.0 ZB=-6. ZT=-4. RADIUS=.5
 PACKAGE WALLOY W=2.0E5
  CYLINDER XC=0.0 YC=0.0 ZB=-10. ZT=-6. RADIUS=.5
 PACKAGE AIR W=2.0E5
  CYLINDER XC=0.0 YC=0.0 ZB=-12. ZT=-10. RADIUS=.5
 PACKAGE WALLOY W=2.0E5
  CYLINDER XC=0.0 YC=0.0 ZB=-16. ZT=-12. RADIUS=.5
 PACKAGE AIR W=2.0E5
  CYLINDER XC=0.0 YC=0.0 ZB=-18. ZT=-16. RADIUS=.5
 PACKAGE WALLOY W=2.0E5
  CYLINDER XC=0.0 YC=0.0 ZB=-22. ZT=-18. RADIUS=.5
 PACKAGE AIR W=2.0E5
  CYLINDER XC=0.0 YC=0.0 ZB=-24. ZT=-22. RADIUS=.5
 PACKAGE WALLOY W=2.0E5
  CYLINDER XC=0.0 YC=0.0 ZB=-28. ZT=-24. RADIUS=.5
 PACKAGE AIR W=2.0E5
  CYLINDER XC=0.0 YC=0.0 ZB=-1.0E20 ZT=-28. RADIUS=.5
 PACKAGE RHA
  BOX X1=-10.0 X2=10.0 Y1=0.0 Y2=10.0 Z1=0.0 Z2=4.0
  XCC=1.7321 YCC=0.0 ZCC=3.86603
  ANGLB=60
 PACKAGE RHA
  BOX X1=-10.0 X2=10.0 Y1=0.0 Y2=10.0 Z1=0.0 Z2=4.0
  XCC=1.7321 YCC=0.0 ZCC=22.02603
  ANGLB=60
 PACKAGE AIR W=1.0E4 BOX FILL
  STATION XS=0. YS=0. ZL=0.
        XS=0. YS=0. ZL=-28.
END
```

KEEL Input For S/D=4 Segmented Penetrator Into T/D=4 Spaced Plates

```
KEEL PROBLEM 7.0001
NM=3 AIR=1 WALLOY=2 RHA=3
DIMEN=3 VISC=1 FLUXER=3 STRESS=1
IMAX=56 JMAX=33 KMAX=348 IQ=55 JQ=32 KQ=347
FAIL=1 STRAIN=1 REZONE=0
NSTN=2 NOP=2000
AREF=.TRUE. BREF=.FALSE. FREF=.FALSE.
LREF=.FALSE. RREF=.FALSE. TREF=.FALSE.
HEADER
 SEGMENTED ROD  L/D = 20  VS = 4.0 KM/SEC  T/D = 4
MESH
CONSTANT SUBGRID NX=30 X0=-2.5 XMAX=2.5 RXNEG=1.1 RXPOS=1.1
          X0LIM=-6.99583 XMLIM=6.99583
          NY=15 Y0=0.0 YMAX=2.5 RYPOS=1.1
          Y0LIM=0. YMLIM=10.85985
          NZ=348 Z0=-37.0 ZMAX=50. RZNEG=1.0
                         RZPOS=1.0
          Z0LIM=-37.0 ZMLIM=50.
GENERATE
 PACKAGE WALLOY W=4.0E5
  CYLINDER XC=0.0 YC=0.0 ZB=-4. ZT=-0.0 RADIUS=.5
 PACKAGE AIR W=4.0E5
  CYLINDER XC=0.0 YC=0.0 ZB=-8. ZT=-4. RADIUS=.5
 PACKAGE WALLOY W=4.0E5
  CYLINDER XC=0.0 YC=0.0 ZB=-12. ZT=-8. RADIUS=.5
 PACKAGE AIR W=4.0E5
  CYLINDER XC=0.0 YC=0.0 ZB=-16. ZT=-12. RADIUS=.5
 PACKAGE WALLOY W=4.0E5
  CYLINDER XC=0.0 YC=0.0 ZB=-20. ZT=-16. RADIUS=.5
 PACKAGE AIR W=4.0E5
  CYLINDER XC=0.0 YC=0.0 ZB=-24. ZT=-20. RADIUS=.5
 PACKAGE WALLOY W=4.0E5
  CYLINDER XC=0.0 YC=0.0 ZB=-28. ZT=-24. RADIUS=.5
 PACKAGE AIR W=4.0E5
  CYLINDER XC=0.0 YC=0.0 ZB=-32. ZT=-28. RADIUS=.5
 PACKAGE WALLOY W=4.0E5
  CYLINDER XC=0.0 YC=0.0 ZB=-36. ZT=-32. RADIUS=.5
 PACKAGE AIR W=4.0E5
  CYLINDER XC=0.0 YC=0.0 ZB=-1.0E20 ZT=-36. RADIUS=.5
 PACKAGE RHA
  BOX X1=-10.0 X2=10.0 Y1=0.0 Y2=10.0 Z1=0.0 Z2=4.0
  XCC=1.7321 YCC=0.0 ZCC=3.86603
  ANGLB=60
 PACKAGE RHA
  BOX X1=-10.0 X2=10.0 Y1=0.0 Y2=10.0 Z1=0.0 Z2=4.0
  XCC=1.7321 YCC=0.0 ZCC=22.02603
  ANGLB=60
 PACKAGE AIR W=1.0E4 BOX FILL
  STATION XS=0. YS=0. ZL=0.
      XS=0. YS=0. ZL=-52.
 END
```

```
NM=3 AIR=1 WALLOY=2 RHA=3
DIMEN=3 VISC=1 FLUXER=3 STRESS=1
IMAX=56 JMAX=33 KMAX=412 IQ=55 JQ=32 KQ=411
FAIL=1 STRAIN=1 REZONE=0
NSTN=2 NOP=2000
AREF=.TRUE. BREF=.FALSE. FREF=.FALSE.
LREF=.FALSE. RREF=.FALSE. TREF=.FALSE.
HEADER
 SEGMENTED ROD  L/D = 20  VS = 4.0 KM/SEC  T/D = 4
MESH
CONSTANT SUBGRID  NX=30 X0=-2.5 XMAX=2.5 RXNEG=1.1 RXPOS=1.1
            X0LIM=-6.99583 XMLIM=6.99583
            NY=15 Y0=0.0 YMAX=2.5 RYPOS=1.1
            Y0LIM=0. YMLIM=10.85985
            NZ=412 Z0=-53.0 ZMAX=50. RZNEG=1.0
                              RZPOS=1.0
            Z0LIM=-53.0 ZMLIM=50.
GENERATE
 PACKAGE WALLOY W=4.0E5
  CYLINDER XC=0.0 YC=0.0 ZB=-4. ZT=-0.0 RADIUS=.5
 PACKAGE AIR W=4.0E5
  CYLINDER XC=0.0 YC=0.0 ZB=-12. ZT=-4. RADIUS=.5
 PACKAGE WALLOY W=4.0E5
  CYLINDER XC=0.0 YC=0.0 ZB=-16. ZT=-12. RADIUS=.5
 PACKAGE AIR W=4.0E5
  CYLINDER XC=0.0 YC=0.0 ZB=-24. ZT=-16. RADIUS=.5
 PACKAGE WALLOY W=4.0E5
  CYLINDER XC=0.0 YC=0.0 ZB=-28. ZT=-24. RADIUS=.5
 PACKAGE AIR W=4.0E5
  CYLINDER XC=0.0 YC=0.0 ZB=-36. ZT=-28. RADIUS=.5
 PACKAGE WALLOY W=4.0E5
  CYLINDER XC=0.0 YC=0.0 ZB=-40. ZT=-36. RADIUS=.5
 PACKAGE AIR W=4.0E5
  CYLINDER XC=0.0 YC=0.0 ZB=-48. ZT=-40. RADIUS=.5
 PACKAGE WALLOY W=4.0E5
  CYLINDER XC=0.0 YC=0.0 ZB=-52. ZT=-48. RADIUS=.5
 PACKAGE AIR W=4.0E5
  CYLINDER XC=0.0 YC=0.0 ZB=-1.0E20 ZT=-52. RADIUS=.5
 PACKAGE RHA
  BOX X1=-10.0 X2=10.0 Y1=0.0 Y2=10.0 Z1=0.0 Z2=4.0
  XCC=1.7321 YCC=0.0 ZCC=3.86603
  ANGLB=60
 PACKAGE RHA
  BOX X1=-10.0 X2=10.0 Y1=0.0 Y2=10.0 Z1=0.0 Z2=4.0
  XCC=1.7321 YCC=0.0 ZCC=22.02603
  ANGLB=60
 PACKAGE AIR W=1.0E4 BOX FILL
  STATION XS=0. YS=0. ZL=0.
          XS=0. YS=0. ZL=-52.
END
```

```
KEEL PROBLEM 8.0000
NM=3 AIR=1 WALLOY=2 RHA=3
DIMEN=3 VISC=1 FLUXER=3 STRESS=1
IMAX=56 JMAX=33 KMAX=360 IQ=55 JQ=32 KQ=359
FAIL=1 STRAIN=1 REZONE=0
NSTN=2 NOP=2000
AREF=.TRUE. BREF=.FALSE. FREF=.FALSE.
LREF=.FALSE. RREF=.FALSE. TREF=.FALSE.
HEADER
 SEGMENTED ROD  L/D = 20  VS = 4.0 KM/SEC  T/D = 4
MESH
CONSTANT SUBGRID NX=30 X0=-2.5 XMAX=2.5 RXNEG=1.1 RXPOS=1.1
              X0LIM=-6.99583 XMLIM=6.99583
              NY=15 Y0=0.0 YMAX=2.5 RYPOS=1.1
              Y0LIM=0. YMLIM=10.85985
              NZ=360 Z0=-40.0 ZMAX=50. RZNEG=1.0
                             RZPOS=1.0
              Z0LIM=-40.0 ZMLIM=50.
GENERATE
 PACKAGE WALLOY W=4.0E5
  CYLINDER XC=0.0 YC=0.0 ZB=-1. ZT=-0.0 RADIUS=.5
 PACKAGE AIR W=4.0E5
  CYLINDER XC=0.0 YC=0.0 ZB=-2. ZT=-1. RADIUS=.5
 PACKAGE WALLOY W=4.0E5
  CYLINDER XC=0.0 YC=0.0 ZB=-3. ZT=-2. RADIUS=.5
 PACKAGE AIR W=4.0E5
  CYLINDER XC=0.0 YC=0.0 ZB=-4. ZT=-3. RADIUS=.5
 PACKAGE WALLOY W=4.0E5
  CYLINDER XC=0.0 YC=0.0 ZB=-5. ZT=-4. RADIUS=.5
 PACKAGE AIR W=4.0E5
  CYLINDER XC=0.0 YC=0.0 ZB=-6. ZT=-5. RADIUS=.5
 PACKAGE WALLOY W=4.0E5
  CYLINDER XC=0.0 YC=0.0 ZB=-7. ZT=-6. RADIUS=.5
 PACKAGE AIR W=4.0E5
  CYLINDER XC=0.0 YC=0.0 ZB=-8. ZT=-7. RADIUS=.5
 PACKAGE WALLOY W=4.0E5
  CYLINDER XC=0.0 YC=0.0 ZB=-9. ZT=-8. RADIUS=.5
 PACKAGE AIR W=4.0E5
  CYLINDER XC=0.0 YC=0.0 ZB=-10. ZT=-9. RADIUS=.5
 PACKAGE WALLOY W=4.0E5
  CYLINDER XC=0.0 YC=0.0 ZB=-11. ZT=-10. RADIUS=.5
 PACKAGE AIR W=4.0E5
  CYLINDER XC=0.0 YC=0.0 ZB=-12. ZT=-11. RADIUS=.5
 PACKAGE WALLOY W=4.0E5
  CYLINDER XC=0.0 YC=0.0 ZB=-13. ZT=-12. RADIUS=.5
 PACKAGE AIR W=4.0E5
  CYLINDER XC=0.0 YC=0.0 ZB=-14. ZT=-13. RADIUS=.5
 PACKAGE WALLOY W=4.0E5
  CYLINDER XC=0.0 YC=0.0 ZB=-15. ZT=-14. RADIUS=.5
 PACKAGE AIR W=4.0E5
  CYLINDER XC=0.0 YC=0.0 ZB=-16. ZT=-15. RADIUS=.5
 PACKAGE WALLOY W=4.0E5
```

```
 CYLINDER XC=0.0 YC=0.0 ZB=-17. ZT=-16. RADIUS=.5
PACKAGE AIR W=4.0E5
 CYLINDER XC=0.0 YC=0.0 ZB=-18. ZT=-17. RADIUS=.5
PACKAGE WALLOY W=4.0E5
 CYLINDER XC=0.0 YC=0.0 ZB=-19. ZT=-18. RADIUS=.5
PACKAGE AIR W=4.0E5
 CYLINDER XC=0.0 YC=0.0 ZB=-20. ZT=-19. RADIUS=.5
PACKAGE WALLOY W=4.0E5
 CYLINDER XC=0.0 YC=0.0 ZB=-21. ZT=-20. RADIUS=.5
PACKAGE AIR W=4.0E5
 CYLINDER XC=0.0 YC=0.0 ZB=-22. ZT=-21. RADIUS=.5
PACKAGE WALLOY W=4.0E5
 CYLINDER XC=0.0 YC=0.0 ZB=-23. ZT=-22. RADIUS=.5
PACKAGE AIR W=4.0E5
 CYLINDER XC=0.0 YC=0.0 ZB=-24. ZT=-23. RADIUS=.5
PACKAGE WALLOY W=4.0E5
 CYLINDER XC=0.0 YC=0.0 ZB=-25. ZT=-24. RADIUS=.5
PACKAGE AIR W=4.0E5
 CYLINDER XC=0.0 YC=0.0 ZB=-26. ZT=-25. RADIUS=.5
PACKAGE WALLOY W=4.0E5
 CYLINDER XC=0.0 YC=0.0 ZB=-27. ZT=-26. RADIUS=.5
PACKAGE AIR W=4.0E5
 CYLINDER XC=0.0 YC=0.0 ZB=-28. ZT=-27. RADIUS=.5
PACKAGE WALLOY W=4.0E5
 CYLINDER XC=0.0 YC=0.0 ZB=-29. ZT=-28. RADIUS=.5
PACKAGE AIR W=4.0E5
 CYLINDER XC=0.0 YC=0.0 ZB=-30. ZT=-29. RADIUS=.5
PACKAGE WALLOY W=4.0E5
 CYLINDER XC=0.0 YC=0.0 ZB=-31. ZT=-30. RADIUS=.5
PACKAGE AIR W=4.0E5
 CYLINDER XC=0.0 YC=0.0 ZB=-32. ZT=-31. RADIUS=.5
PACKAGE WALLOY W=4.0E5
 CYLINDER XC=0.0 YC=0.0 ZB=-33. ZT=-32. RADIUS=.5
PACKAGE AIR W=4.0E5
 CYLINDER XC=0.0 YC=0.0 ZB=-34. ZT=-33. RADIUS=.5
PACKAGE WALLOY W=4.0E5
 CYLINDER XC=0.0 YC=0.0 ZB=-35. ZT=-34. RADIUS=.5
PACKAGE AIR W=4.0E5
 CYLINDER XC=0.0 YC=0.0 ZB=-36. ZT=-35. RADIUS=.5
PACKAGE WALLOY W=4.0E5
 CYLINDER XC=0.0 YC=0.0 ZB=-37. ZT=-36. RADIUS=.5
PACKAGE AIR W=4.0E5
 CYLINDER XC=0.0 YC=0.0 ZB=-38. ZT=-37. RADIUS=.5
PACKAGE WALLOY W=4.0E5
 CYLINDER XC=0.0 YC=0.0 ZB=-39. ZT=-38. RADIUS=.5
PACKAGE AIR W=4.0E5
 CYLINDER XC=0.0 YC=0.0 ZB=-1.0E20 ZT=-39. RADIUS=.5
PACKAGE RHA
 BOX X1=-10.0 X2=10.0 Y1=0.0 Y2=10.0 Z1=0.0 Z2=4.0
 XCC=1.7321 YCC=0.0 ZCC=3.86603
 ANGLB=60
PACKAGE RHA
 BOX X1=-10.0 X2=10.0 Y1=0.0 Y2=10.0 Z1=0.0 Z2=4.0
 XCC=1.7321 YCC=0.0 ZCC=22.02603
```

```
  ANGLB=60
 PACKAGE AIR W=1.0E4 BOX FILL
  STATION XS=0. YS=0. ZL=0.
       XS=0. YS=0. ZL=-40.
END
```

APPENDIX B - Material Properties

APPENDIX B

Material Properties and Equation of State Data

	RHA	TUNGSTEN
Ambient density (g/cc)	7.86	17.3
Ambient sound speed (cm/s)	4.61e5	4.0e5
Shock velocity/particle velocity slope	1.73	1.268
Initial Gruneisen ratio	1.67	1.43
Minimum Pressure (dynes/cm**2)	-1.0e20	-10.e9
Poisson's ratio	0.26	0.3
Atomic weight	55.85	184.
DeBye's temperature (K)	355	270
Vapor coefficient	0.25	0.2
Ambient energy per unit mass (ergs/g)	0.0	0.0
Ambient melt energy per unit mass (ergs/g)	7.4e9	4.77e9
Fusion energy per unit mass (ergs/g)	2.74e9	1.84e9
Sublimation energy per unit mass (ergs/g)	74.2e9	46.e9
Ambient vaporization energy per unit mass (ergs/g)	22.4e9	13.6e9
Ambient energy per unit mass at end of vaporization (ergs/g)	86.8e9	58.4e9
Initial yield strength (dynes/cm**2)	15.e9	20.e9
Saturation yield strength (dynes/cm**2)	15.e9	20.e9
Plastic strain at saturation yield strength	0.3	0.3
Yield strength ratio for first point on thermal softening curve	0.9	0.9
Energy ratio for first point on thermal softening curve	0.5	0.5
Yield strength ratio for second point on thermal softening curve	0.9	0.9
Energy ratio for second point on thermal softening curve	0.5	0.5
Second coefficient in Hugoniot pressure curve (dynes/cm**2)	4.21968e12	4.6987e12
Third coefficient in Hugoniot pressure curve (dynes/cm**2)	5.12915e12	3.345e12
Ultimate failure stress (dynes/cm**2)	42.e9	1.e50
Ultimate failure strain	1.75	0.14

APPENDIX C - Plots Used For Residual Mass Calculations

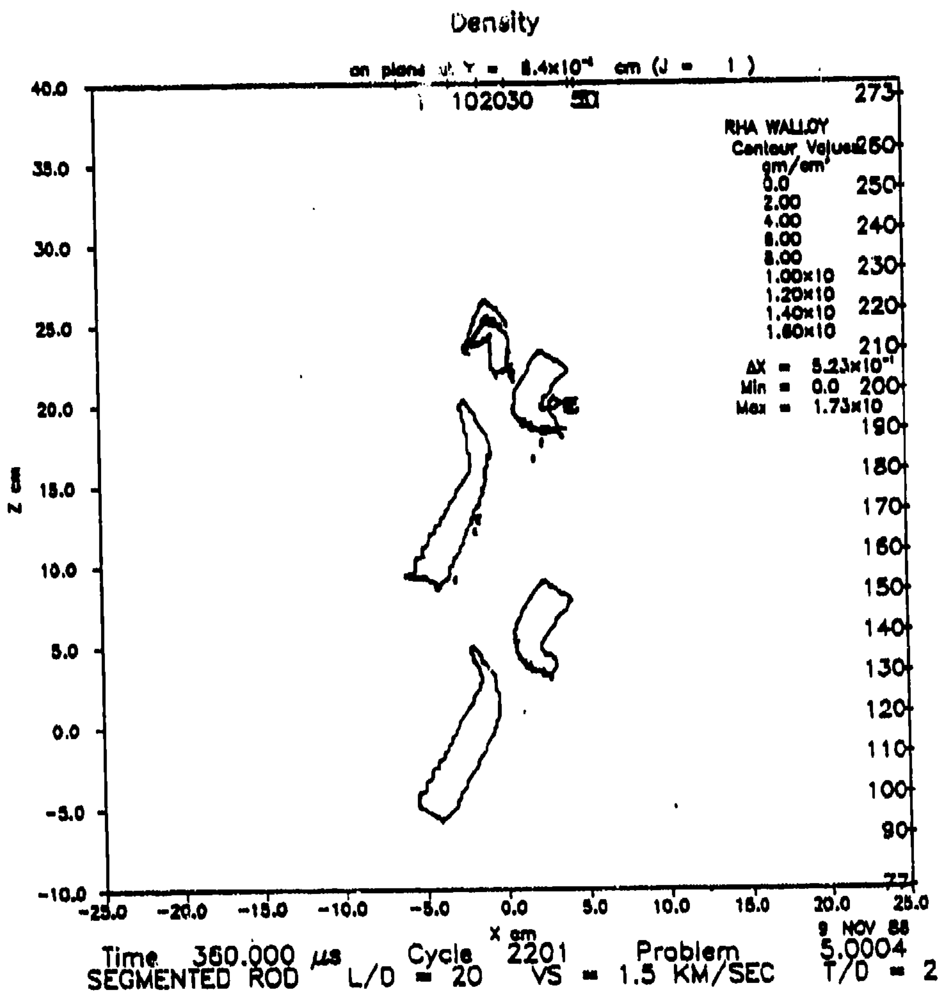

Density
on plane at Y = 8.4x10⁻⁴ cm (J = 1)
102030 50
RHA WALLOY
Contour Values
gm/cm³
0.0
2.00
4.00
6.00
8.00
1.00x10
1.20x10
1.40x10
1.60x10
ΔX = 5.23x10⁻¹
Min = 0.0
Max = 1.73x10
Z cm
X cm
9 NOV 88
Time 360.000 μs Cycle 2201 Problem 5.0004
SEGMENTED ROD L/D = 20 VS = 1.5 KM/SEC T/D = 2

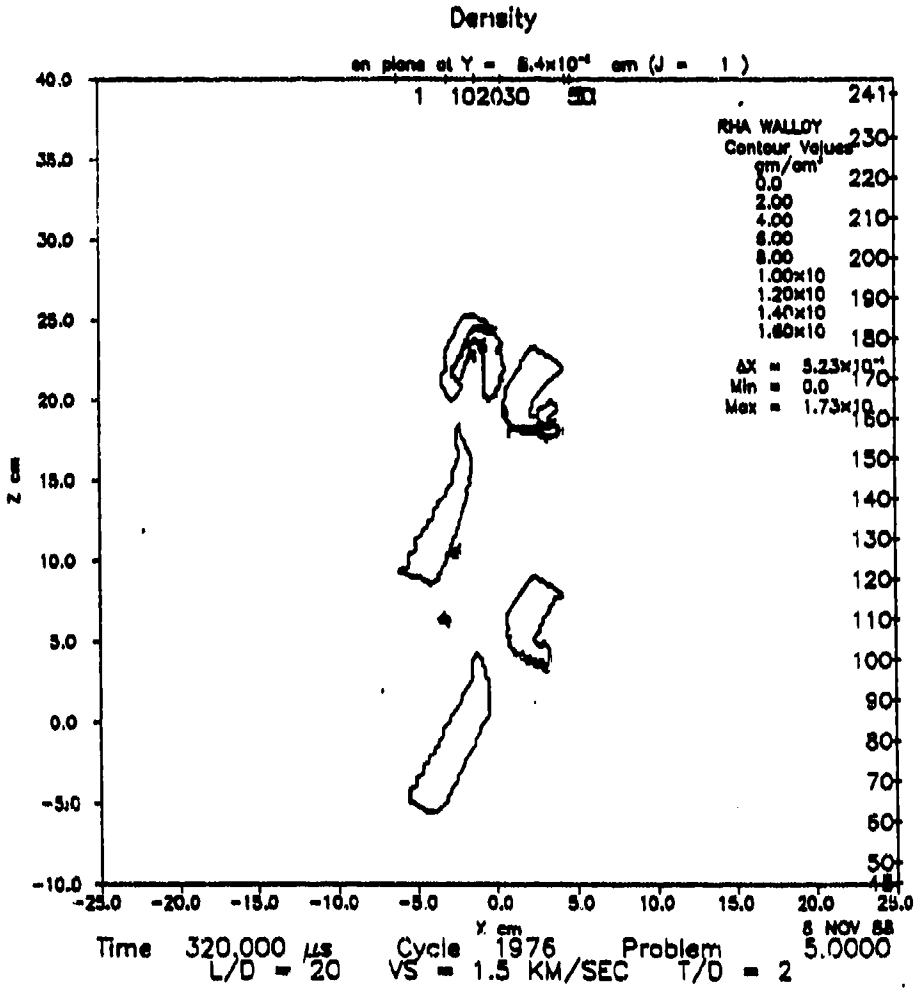

Density
on plane at Y = 8.4x10⁻⁴ cm (J = 1)
1 102030 50
RHA WALLOY
Contour Values
gm/cm³
0.0
2.00
4.00
6.00
8.00
1.00x10
1.20x10
1.40x10
1.60x10
ΔX = 5.23x10⁻¹
Min = 0.0
Max = 1.73x10
Z cm
X cm
8 NOV 88
Time 320,000 μs Cycle 1976 Problem 5.0000
L/D = 20 VS = 1.5 KM/SEC T/D = 2

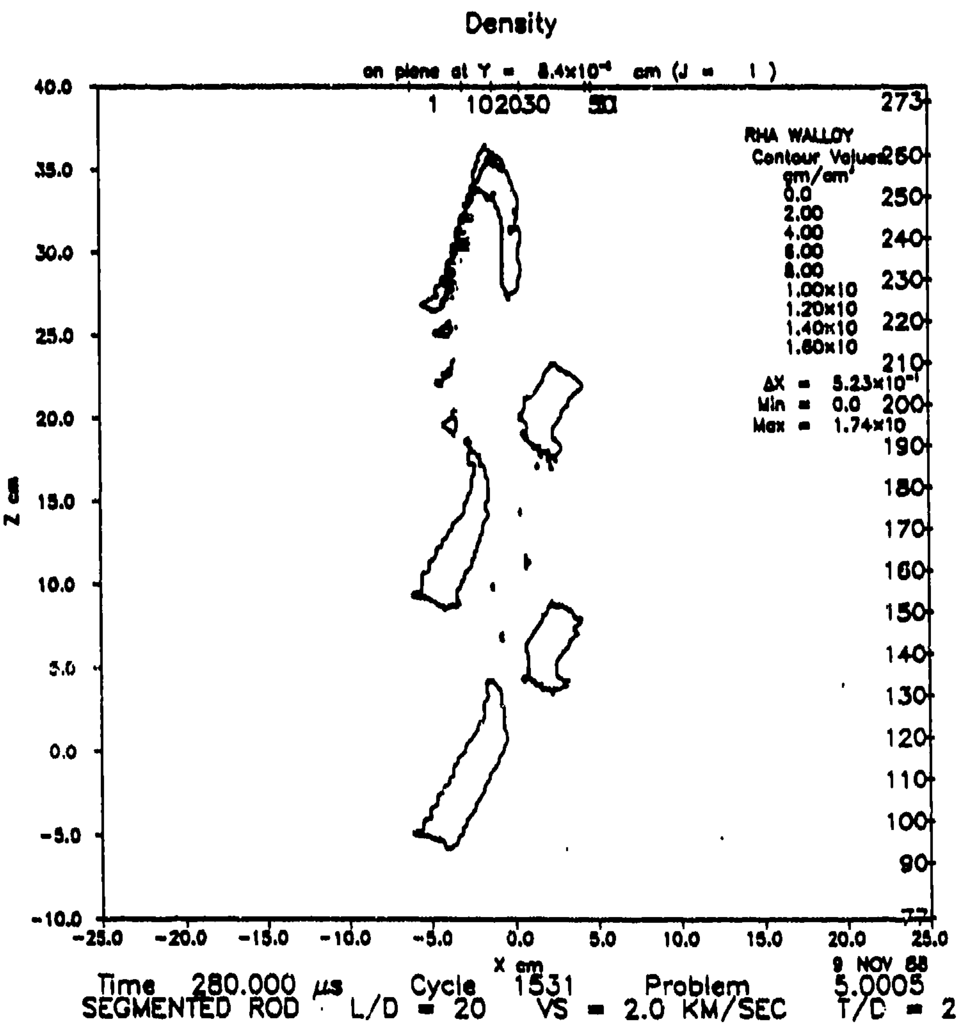
Density
on plane at Y = 8.4x10⁻⁴ cm (J = 1)
RHA WALLOY
Contour Values
gm/cm³
0.0
2.00
4.00
6.00
8.00
1.00x10
1.20x10
1.40x10
1.60x10
ΔX = 5.23x10⁻¹
Min = 0.0
Max = 1.74x10
Z cm
X cm
9 NOV 88
Time 280.000 μs Cycle 1531 Problem 5.0005
SEGMENTED ROD L/D = 20 VS = 2.0 KM/SEC T/D = 2

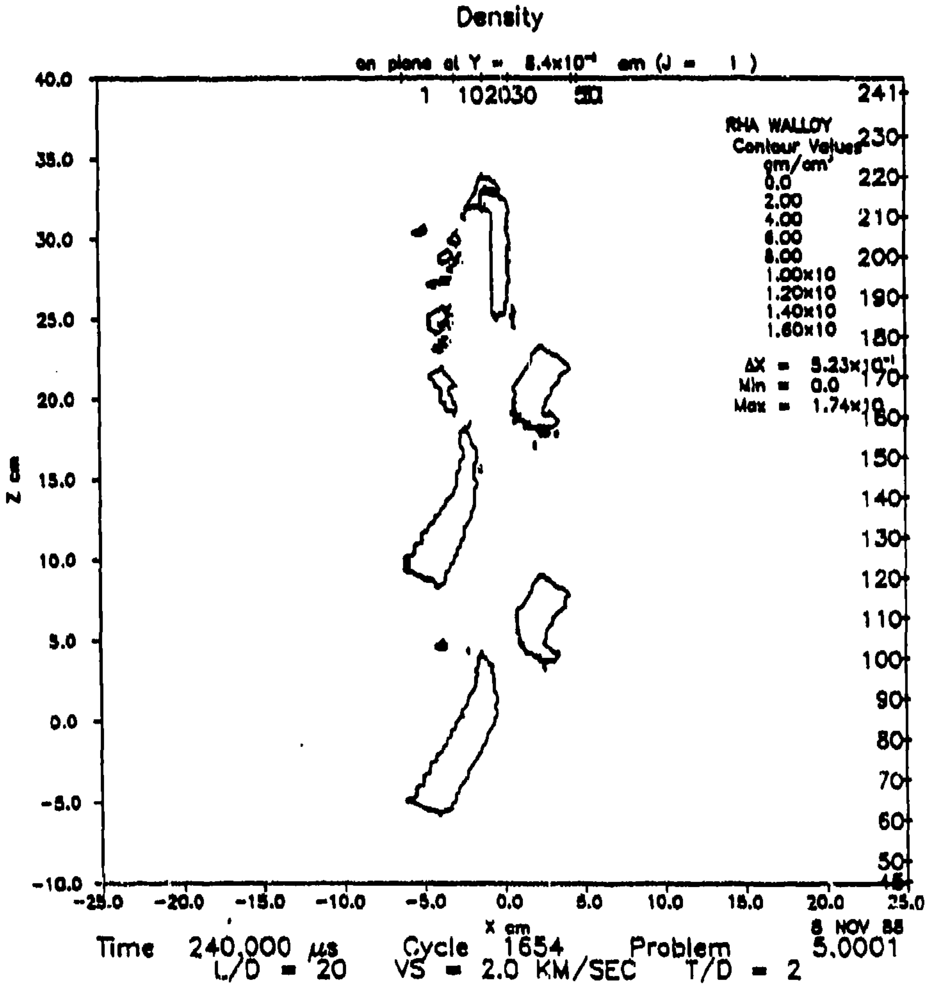

Density
on plane at Y = 8.4x10⁻¹ cm (J = 1)
1 102030
RHA WALLOY
Contour Values
gm/cm³
0.0
2.00
4.00
6.00
8.00
1.00x10
1.20x10
1.40x10
1.60x10
ΔX = 5.23x10⁻¹
Min = 0.0
Max = 1.74x10
Z cm
X cm
8 NOV 88
Time 240.000 µs Cycle 1654 Problem 5.0001
L/D = 20 VS = 2.0 KM/SEC T/D = 2

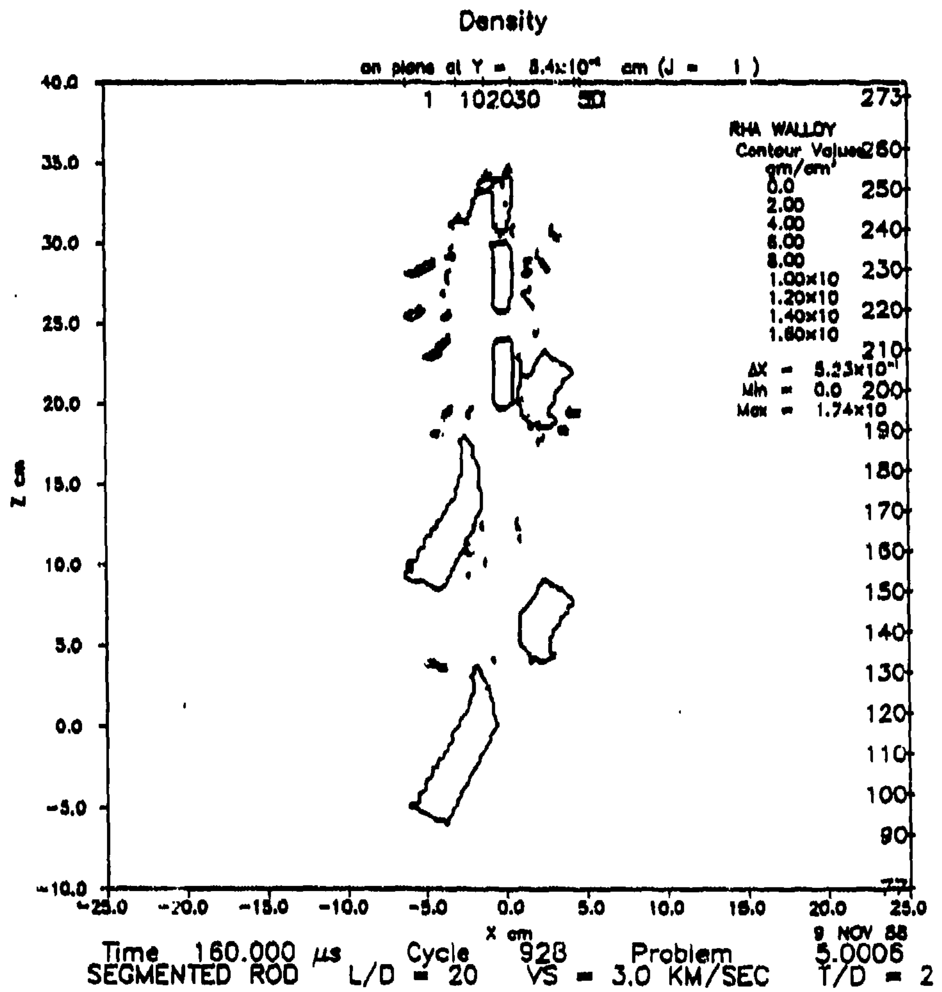
Density
1 102030 50
273
RHA WALLOY
Contour Values
0.0
2.00
4.00
6.00
8.00
1.00x10
1.20x10
1.40x10
1.60x10
Min = 0.0
Max = 1.74x10
Z cm
X cm
9 NOV 88
Time 160.000 µs Cycle 928 Problem 5.0006
SEGMENTED ROD L/D = 20 VS = 3.0 KM/SEC T/D = 2

Density

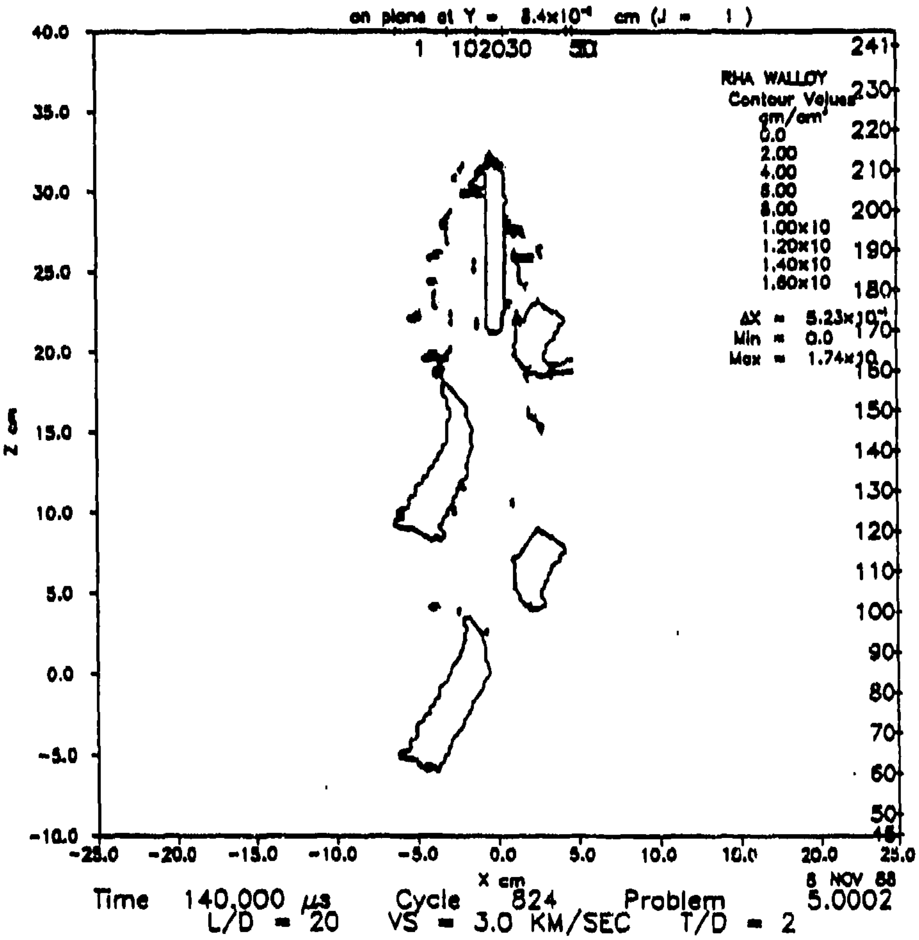
on plane at Y = 8.4x10⁻⁴ cm (J = 1)
1 102030 50
RHA WALLOY
Contour Values gm/cm³
0.0
2.00
4.00
6.00
8.00
1.00x10
1.20x10
1.40x10
1.60x10
ΔX = 5.23x10⁻¹
Min = 0.0
Max = 1.74x10
Z cm
X cm
8 NOV 88
Time 140.000 μs Cycle 824 Problem 5.0002
L/D = 20 VS = 3.0 KM/SEC T/D = 2

Density

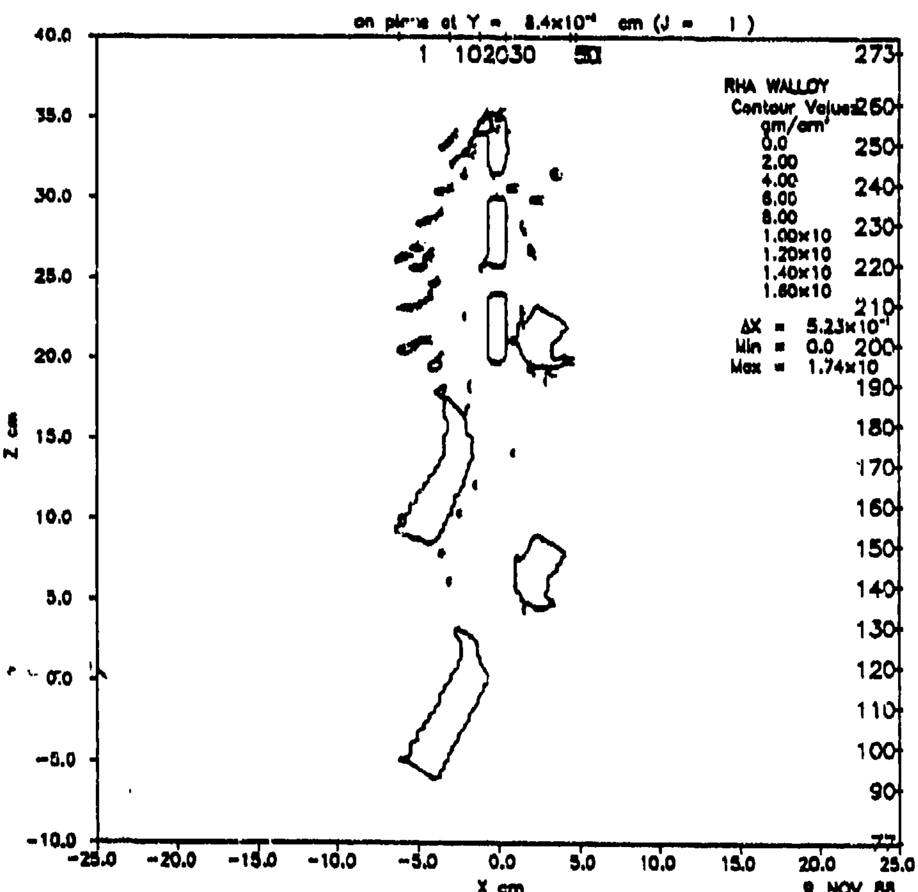

Time 120.000 μs Cycle 741 Problem 5.0007
SEGMENTED ROD L/D = 20 VS = 4.0 KM/SEC T/D = 2

Density

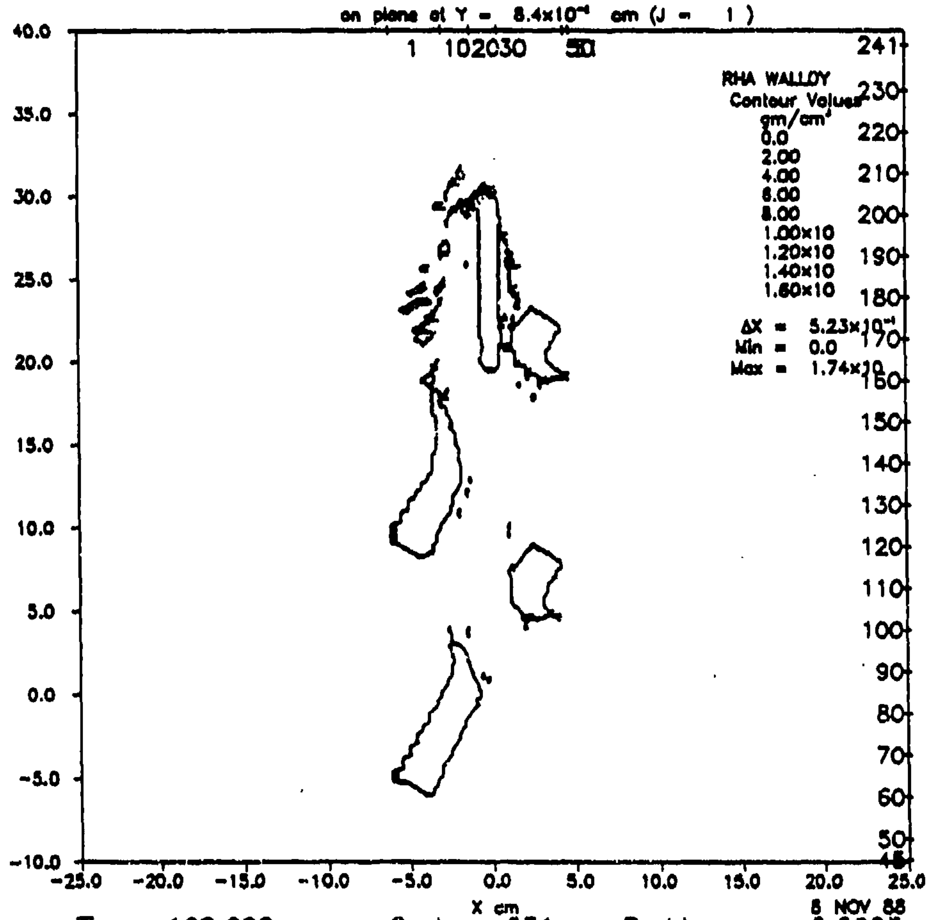

Time 100,000 μs Cycle 631 Problem 5.0003
L/D = 20 VS = 4.0 KM/SEC T/D = 2

Density

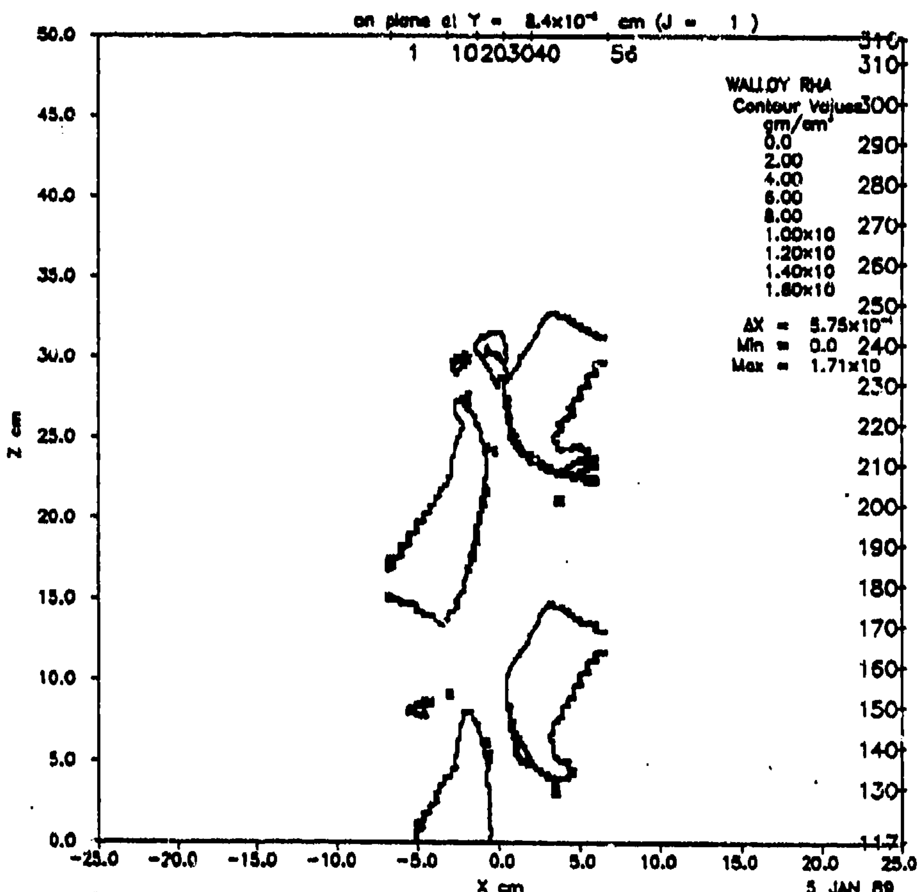

Time 360.194 µs Cycle 1977 Problem 518.8800
SEGMENTED ROD L/D = 20 VS = 2.0 KM/SEC T/D = 4

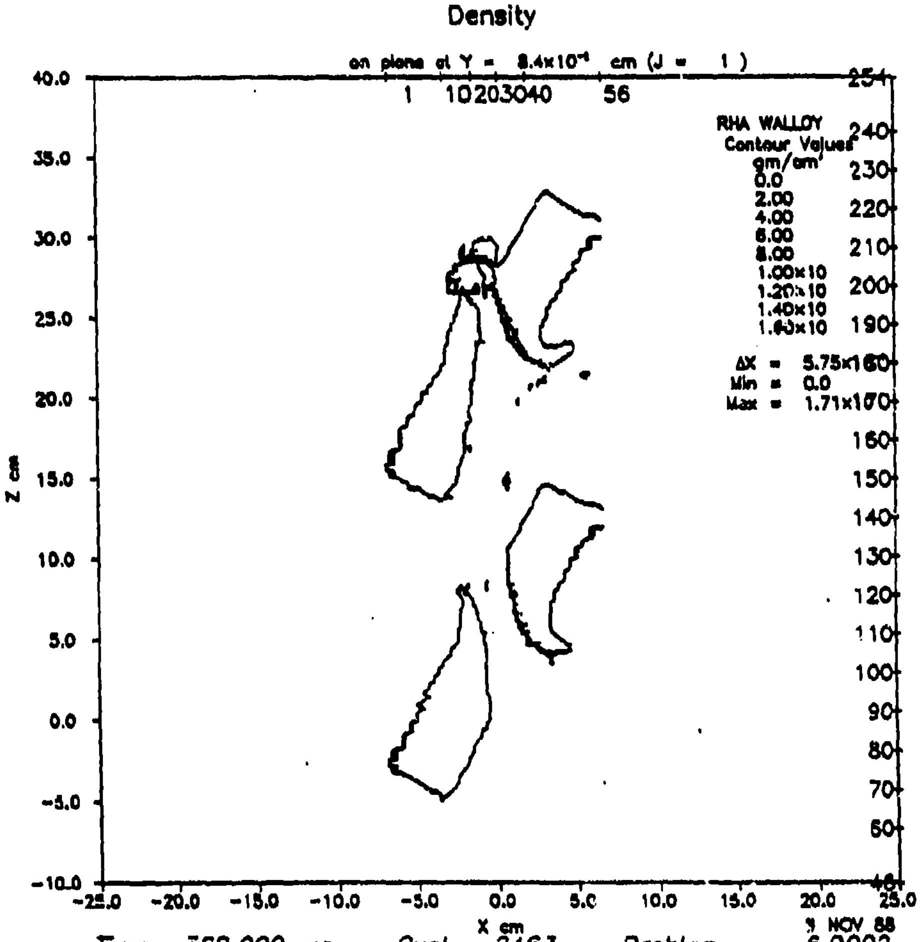

Time 360.000 μs Cycle 2463 Problem 6.0002
L/D = 20 VS = 2.0 KM/SEC T/D = 4

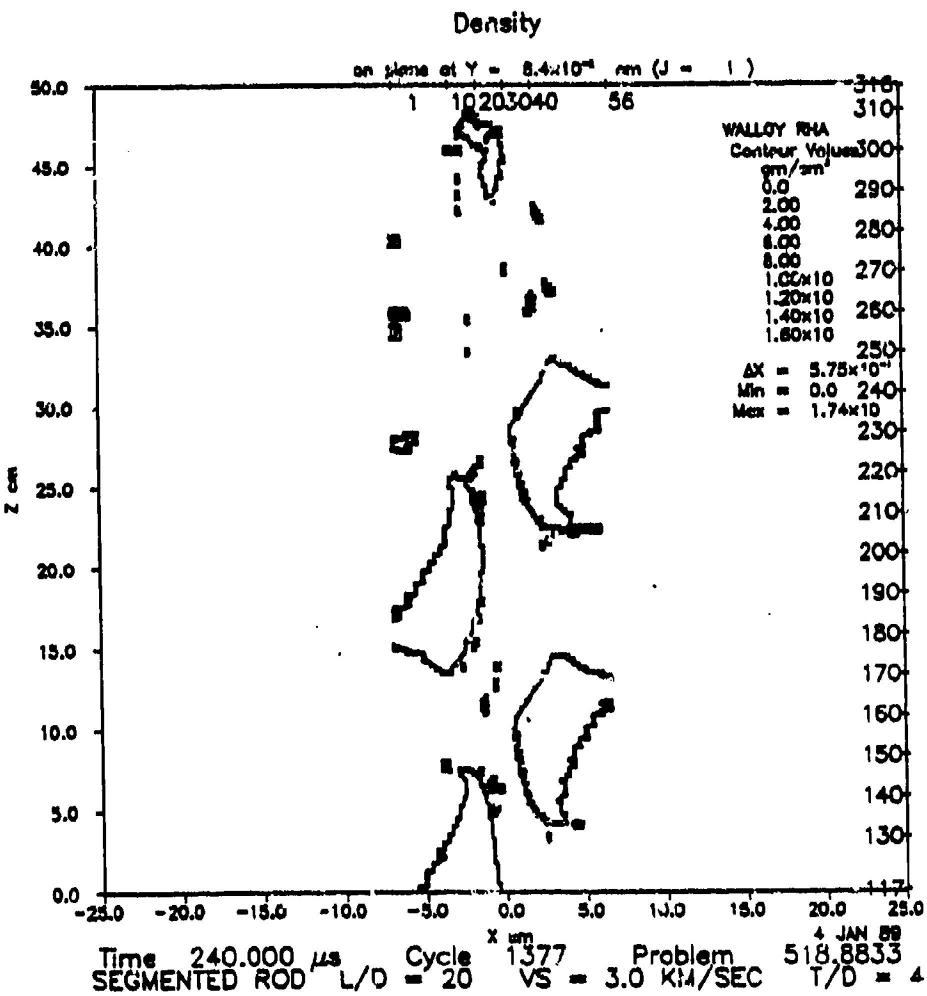
Density
on plane at Y = 8.4x10⁻⁴ cm (J = 1)
1 10203040 56
WALLOY RHA
Contour Values
gm/cm³
0.0
2.00
4.00
6.00
8.00
1.00x10
1.20x10
1.40x10
1.60x10
ΔX = 5.75x10⁻¹
Min = 0.0
Max = 1.74x10
50.0
45.0
40.0
35.0
30.0
25.0
20.0
15.0
10.0
5.0
0.0
Z cm
-25.0
-20.0
-15.0
-10.0
-5.0
0.0
5.0
10.0
15.0
20.0
25.0
X cm
310
300
290
280
270
260
250
240
230
220
210
200
190
180
170
160
150
140
130
117
4 JAN 89
Time 240.000 μs Cycle 1377 Problem 518.8833
SEGMENTED ROD L/D = 20 VS = 3.0 KM/SEC T/D = 4

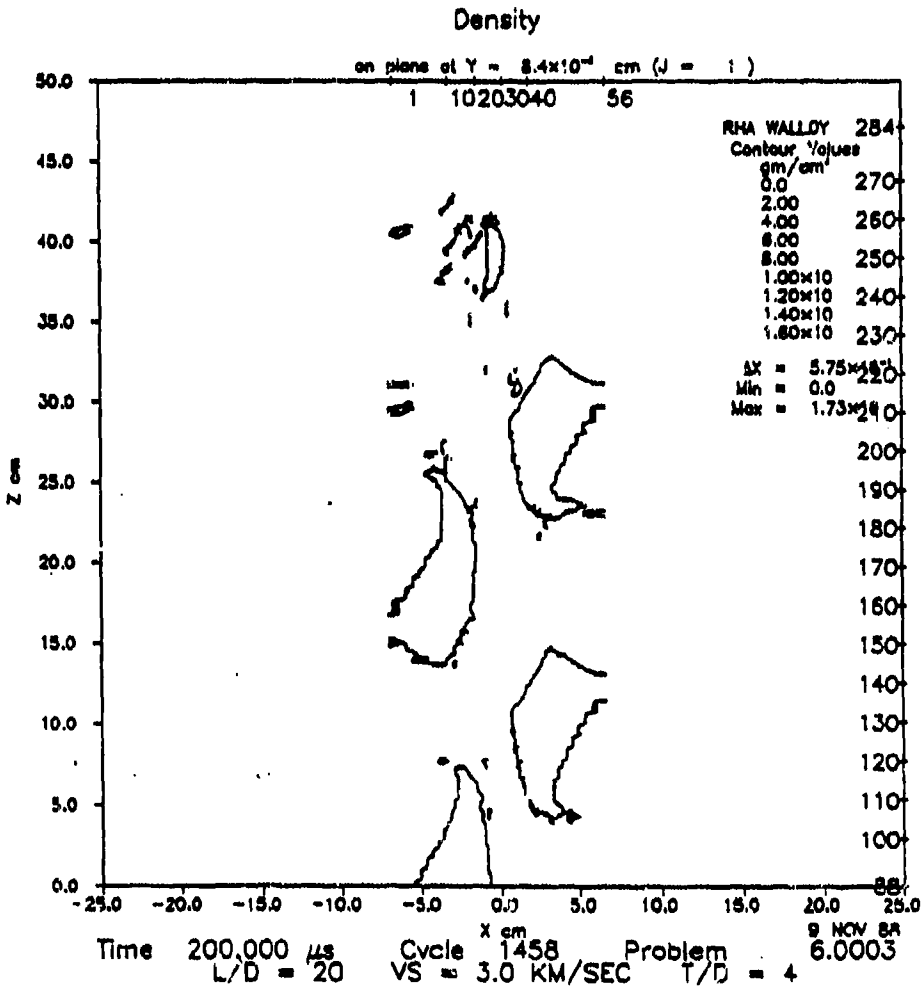

Density
on plane at Y = 8.4×10⁻¹ cm (J = 1)
1 10203040 56
RHA WALLOY
Contour Values
gm/cm³
0.0
2.00
4.00
6.00
8.00
1.00×10
1.20×10
1.40×10
1.60×10
Min = 0.0
Z cm
X cm
9 NOV 88
Time 200.000 μs Cycle 1458 Problem 6.0003
L/D = 20 VS = 3.0 KM/SEC T/D = 4

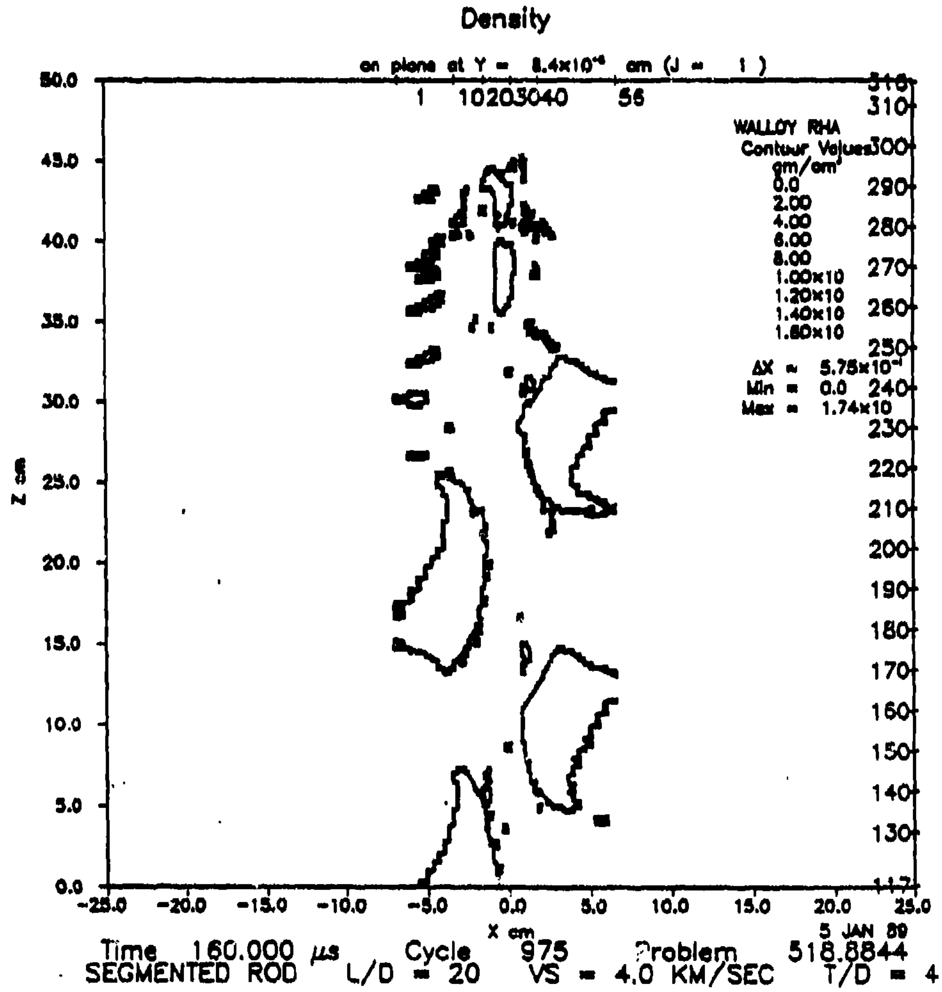
Density
on plane at Y = 8.4x10⁻⁶ cm (J = 1)
1 10203040 56
WALLOY RHA
Contour Values
gm/cm³
0.0
2.00
4.00
6.00
8.00
1.00x10
1.20x10
1.40x10
1.60x10
ΔX = 5.75x10⁻¹
Min = 0.0
Max = 1.74x10
Z cm
X cm
5 JAN 89
Time 160.000 µs Cycle 975 Problem 518.8844
SEGMENTED ROD L/D = 20 VS = 4.0 KM/SEC T/D = 4

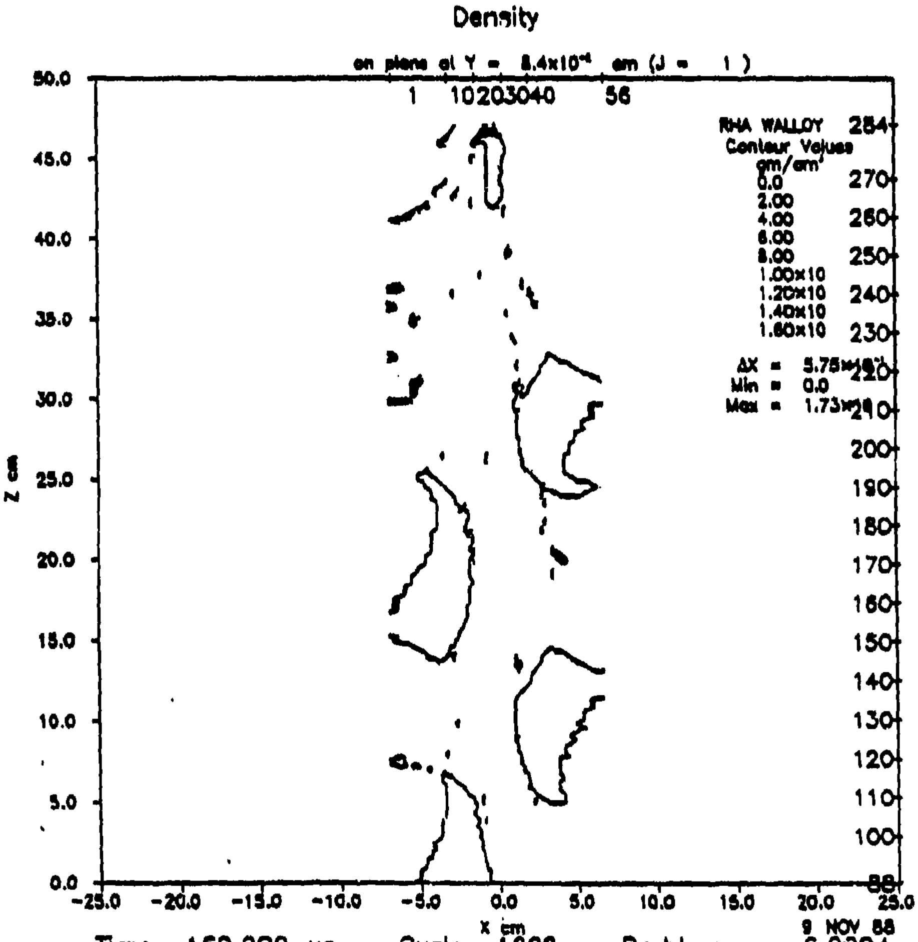

Time 160.000 μs Cycle 1228 Problem 6.0004
L/D = 20 VS = 4.0 KM/SEC T/D = 4

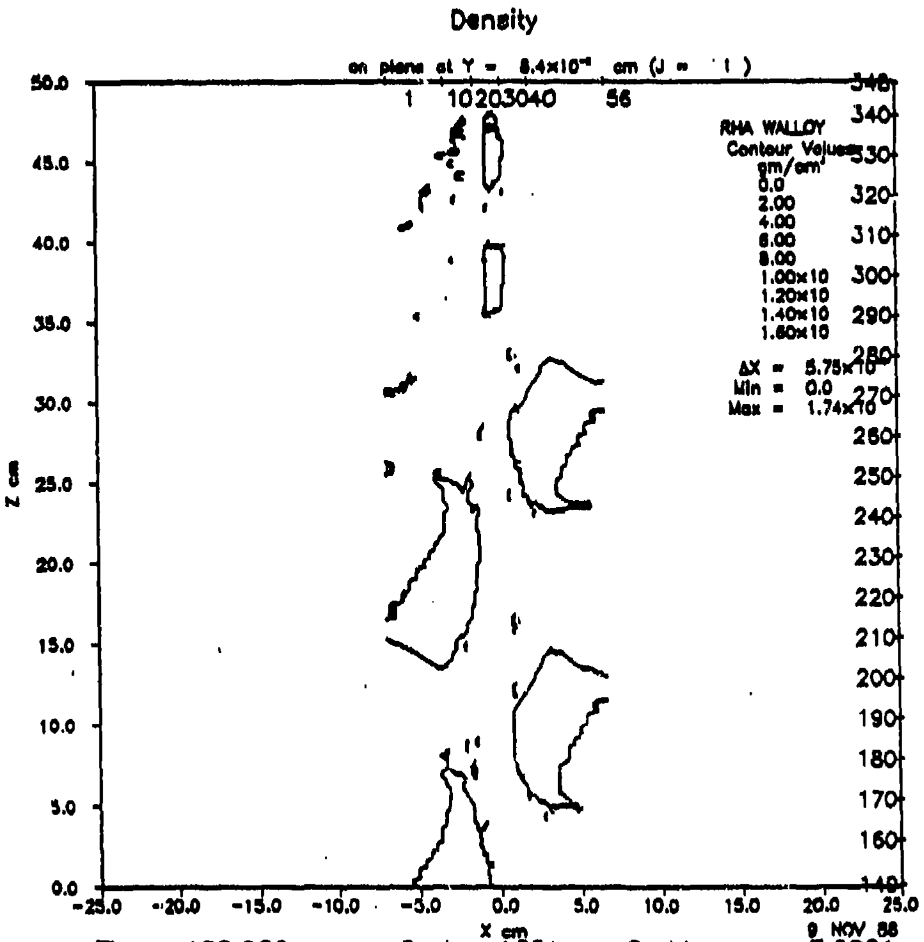

Time 180.000 μs Cycle 1351 Problem 7.0001
SEGMENTED ROD L/D = 20 VS = 4.0 KM/SEC T/D = 4

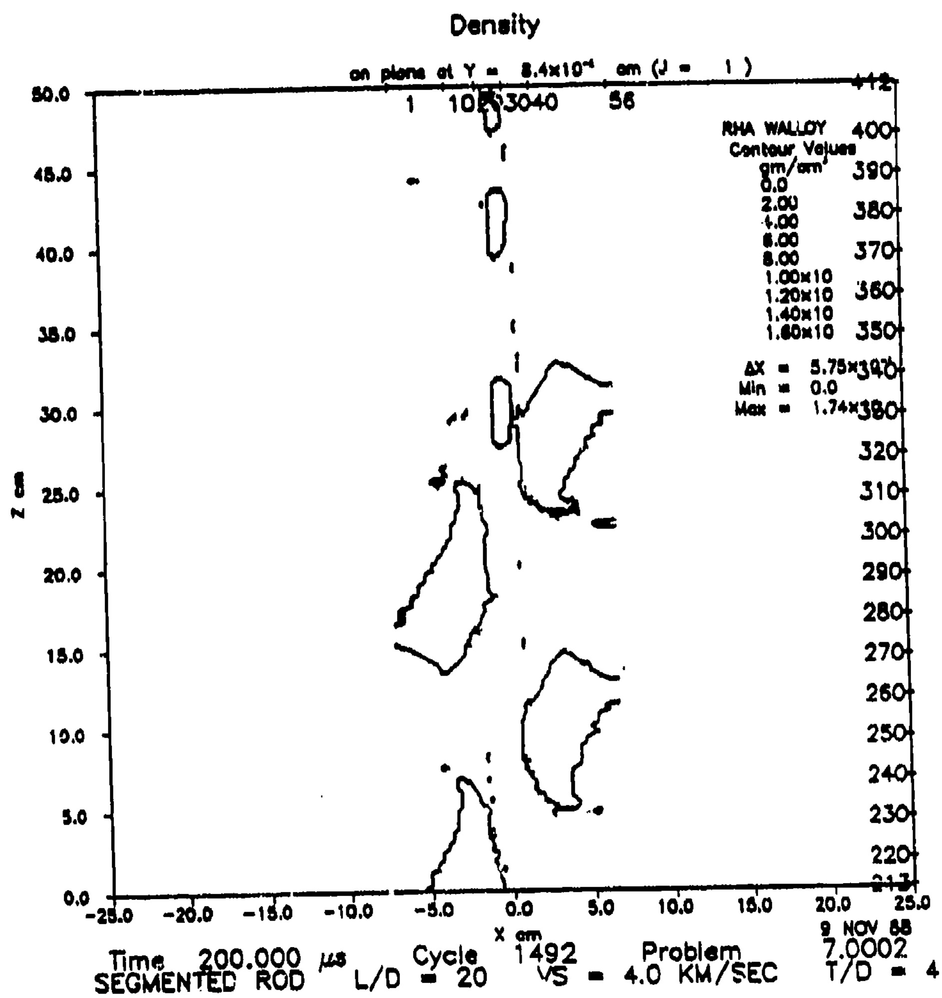
Density
on plane at Y = 8.4x10⁻⁴ cm (J = 1)
RHA WALLOY
Contour Values
gm/cm³
0.0
2.00
4.00
6.00
8.00
1.00x10
1.20x10
1.40x10
1.60x10
Min = 0.0
Z cm
X cm
9 NOV 88
Time 200.000 μs Cycle 1492 Problem 7.0002
SEGMENTED ROD L/D = 20 VS = 4.0 KM/SEC T/D = 4

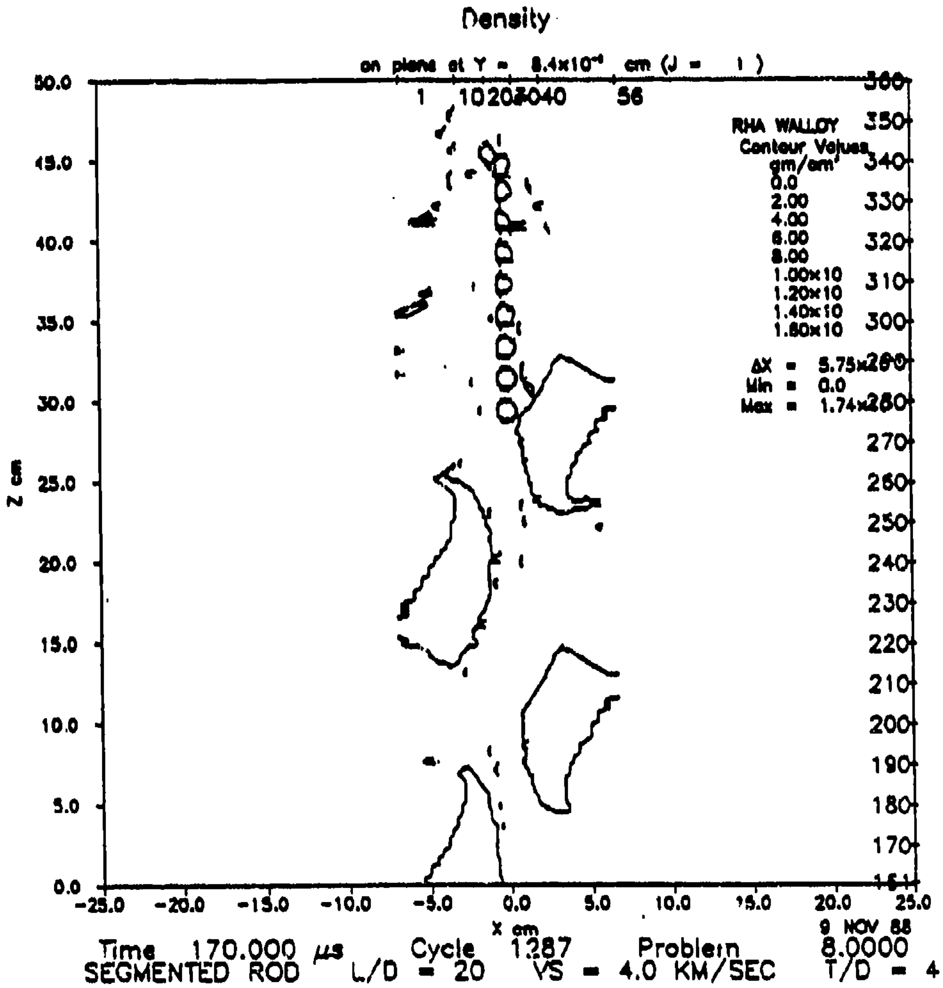
Density
on plane at Y = 8.4x10⁻¹ cm (J = 1)
RHA WALLOY
Contour Values gm/cm³
0.0
2.00
4.00
6.00
8.00
1.00x10
1.20x10
1.40x10
1.60x10
ΔX = 5.75x10⁻¹
Min = 0.0
Max = 1.74x10
Z cm
X cm
9 NOV 88
Time 170.000 µs Cycle 1287 Problem 8.0000
SEGMENTED ROD L/D = 20 VS = 4.0 KM/SEC T/D = 4

No of Copies	Organization
(Unclass., unlimited) 12 (Unclass., limited) 2 (Classified) 2	Administrator Defense Technical Info Center ATTN: DTIC-DDA Cameron Station Alexandria, VA 22304-6145
1	HQDA (SARD-TR) WASH DC 20310-0001
1	Commander US Army Materiel Command ATTN: AMCDRA-ST 5001 Eisenhower Avenue Alexandria, VA 22333-0001
1	Commander US Army Laboratory Command ATTN: AMSLC-DL Adelphi, MD 20783-1145
2	Commander Armament RD&E Center US Army AMCCOM ATTN: SMCAR-MSI Picatinny Arsenal, NJ 07806-5000
2	Commander Armament RD&E Center US Army AMCCOM ATTN: SMCAR-TDC Picatinny Arsenal, NJ 07806-5000
1	Director Benet Weapons Laboratory Armament RD&E Center US Army AMCCOM ATTN: SMCAR-LCB-TL Watervliet, NY 12189-4050
1	Commander US Army Armament, Munitions and Chemical Command ATTN: SMCAR-ESP-L Rock Island, IL 61299-5000
1	Commander US Army Aviation Systems Command ATTN: AMSAV-DACL 4300 Goodfellow Blvd. St. Louis, MO 63120-1798
1	Director US Army Aviation Research and Technology Activity Ames Research Center Moffett Field, CA 94035-1099

No of Copies	Organization
1	Commander US Army Missile Command ATTN: AMSMI-RD-CS-R (DOC) Redstone Arsenal, AL 35898-5010
1	Commander US Army Tank Automotive Command ATTN: AMSTA-TSL (Technical Library) Warren, MI 48397-5000
1	Director US Army TRADOC Analysis Command ATTN: ATAA-SL White Sands Missile Range, NM 88002-5502
(Class. only) 1	Commandant US Army Infantry School ATTN: ATSH-CD (Security Mgr.) Fort Benning, GA 31905-5660
(Unclass. only) 1	Commandant US Army Infantry School ATTN: ATSH-CD-CSO-OR Fort Benning, GA 31905-5660
(Class. only) 1	The Rand Corporation P.O. Box 2138 Santa Monica, CA 90401-2138
1	Air Force Armament Laboratory ATTN: AFATL/DLODL Eglin AFB, FL 32542-5000

Aberdeen Proving Ground

Dir, USAMSAA
ATTN: AMXSY-D
AMXSY-MP, H. Cohen
Cdr, USATECOM
ATTN: AMSTE-TO-F
Cdr, CRDEC, AMCCOM
ATTN: SMCCR-RSP-A
SMCCR-MU
SMCCR-MSI
Dir, VLAMO
ATTN: AMSLC-VL-D

No. of Copies	Organization
4	Commander Naval Surface Warfare Center ATTN: Paula Walter Kenneth Kiddy F. J. Zerilla Lisa Meusi 10901 New Hampshire Avenue Silver Spring, MD 20903-5000
2	AFATL/DLJW ATTN: Dr. W. Cook M. Nixon Eglin AFB, FL 32542
4	Los Alamos National Laboratory ATTN: Dr. E. Cort Dr. R. Fujita Dr. R. Karpp (MS P940) Dr. M. Burkett P.O. Box 1663 Los Alamos, NM 87545
3	Sandia National Laboratory ATTN: M. Kipp P. Yarrington W. Herrmann (Org. 150) Albuquerque, NM 87115
2	Orlando Technology Inc. ATTN: Mr. D. Matuska Mr. J. Osborne P.O. Box 855 60 Second Street Shalimar, FL 32579
1	General Research Corporation ATTN: Dr. A. Charters P.O. Box 6770 5383 Hollister Avenue Santa Barbara, CA 93160-6770
1	General Dynamics ATTN: J. H. Cuadros P.O. Box 2507 Pomona, CA 91745
2	Honeywell Inc. ATTN: Dr. G. Johnson R. Stryk 7225 Northland Drive Brooklyn Park, MN 55428

No. of Copies	Organization
1	Systems, Science and Software ATTN: Dr. R. Sedgwick La Jolla, CA 92038
1	Orlando Technology Inc. ATTN: Mr. N. Piburn 2340 Alamo SE, Suite 101 Albuquerque, NM 87106

USER EVALUATION SHEET/CHANGE OF ADDRESS

This Laboratory undertakes a continuing effort to improve the quality of the reports it publishes. Your comments/answers to the items/questions below will aid us in our efforts.

1. BRL Report Number BRL-TR-3080 Date of Report February 1990

2. Date Report Received ____________

3. Does this report satisfy a need? (Comment on purpose, related project, or other area of interest for which the report will be used.) ____________

4. How specifically, is the report being used? (Information source, design data, procedure, source of ideas, etc.) ____________

5. Has the information in this report led to any quantitative savings as far as man-hours or dollars saved, operating costs avoided or efficiencies achieved, etc? If so, please elaborate. ____________

6. General Comments. What do you think should be changed to improve future reports? (Indicate changes to organization, technical content, format, etc.) ____________

CURRENT ADDRESS

Name ____________

Organization ____________

Address ____________

City, State, Zip ____________

7. If indicating a Change of Address or Address Correction, please provide the New or Correct Address in Block 6 above and the Old or Incorrect address below.

OLD ADDRESS

Name ____________

Organization ____________

Address ____________

City, State, Zip ____________

(Remove this sheet, fold as indicated, staple or tape closed, and mail.)

FOLD HERE

Director
U.S. Army Ballistic Research Laboratory
ATTN: SLCBR-DD-T
Aberdeen Proving Ground, MD 21005-5066

OFFICIAL BUSINESS

NO POSTAGE
NECESSARY
IF MAILED
IN THE
UNITED STATES

BUSINESS REPLY MAIL
FIRST CLASS PERMIT NO 12062 WASHINGTON,DC

POSTAGE WILL BE PAID BY DEPARTMENT OF THE ARMY

Director
U.S. Army Ballistic Research Laboratory
ATTN: SLCBR-DD-T
Aberdeen Proving Ground, MD 21005-9989

FOLD HERE